Chapter 6 Small Amplitude Studies in Structures

6.1 Introduction

The past few years have seen a proliferation of real-time structural monitoring testbeds. Analysis of the resulting data is leading towards a better understanding of building response. Current research at the California Institute of Technology into ambient, forced (Bradford et al, 2004) and earthquake vibration analysis of large concrete buildings, concrete dams (Alves and Hall, 2003) and wood-frame buildings (Camelo, 2003) indicates that during small shaking events, there is a measurable change in recorded natural frequencies of all these types of structures. In the case of wood-frame structures, natural frequencies may be reduced by a factor of two during stronger shaking, even without identifiable structural damage (Camelo, 2003). This non-linear structural softening is not well characterised or understood, and needs to be accounted for if real-time building monitoring is to be used effectively as a post-earthquake damage assessment tool.

This Chapter attempts to document the amount of frequency shifting in the instrumented large structures at the campus of the California Institute of Technology. The current state of instrumentation on campus is described, and the observed changes in fundamental frequencies are correlated with weather, earthquake history, and building usage.

The wandering of the natural frequencies of the Robert A. Millikan Library on the campus of the California Institute of Technology (Caltech) has been previously documented (Kuroiwa, 1967; Trifunac, 1972; Foutch, 1976; Luco et al, 1987; Chopra, 1995). Since its construction in 1967, a decrease in these resonant frequencies may be observed from yearly forced vibration experiments and from strong motion records. This frequency drop has been interpreted to be due to a corresponding softening in system stiffness. Recent ambient and forced vibration tests indicate the fundamental natural frequency of the structure is now approximately 21% lower in the East-West direction and 12% lower in the North-South direction than was determined shortly after construction (Kuroiwa, 1967). Strong motion records indicate that the natural frequencies drop even further during moderately large events. In one such example, the M6.1 Whittier Narrows earthquake, located 19*km* from the library, the E-W and N-S natural frequencies decreased by 17% and 25% respectively, compared with forced vibration measurements prior to the event (Levine et al, 1988). The structure recovers stiffness somewhat after a moderately large shaking event, but due to lack of data in the immediate aftermath of these mainshocks, the recovery time-frame cannot be constrained. Further, Kuroiwa (1967) and others noted that the resonant frequencies drop measurably when the applied force during forced vibrations is increased — in 1966 during construction the fundamental E-W frequency dropped 3% when applied force was increased by a factor of 8.

Recent improvements in the quality and quantity of instrumentation in the building and at other sites on the Caltech campus have led to renewed investigation of the structure. Analysis of structural response to previously un-recorded ambient and small intensity ground motions are now possible.

Data is presented which indicates that not only do the natural frequencies change significantly during strong shaking — as evidenced by analogue recordings of large earthquakes in the recent past — but there are also measurable changes in the resonant frequencies of the buildings due to —

- forced vibrations using varying forces
- minor earthquake shaking
- weather conditions (rain and wind events, extremes in temperature)

These last two factors are shown to also affect the recently constructed Broad Center on the Caltech campus (the Broad Center has not yet been shaken, or subjected to strong earthquake motions).

The lowering of the natural frequencies during transient events in Millikan Library is likely due to a combination of two mechanisms, a non-linear softening of the superstructure itself, as well as an interaction of the structure with the surrounding soil. Changes in occupancy usage are also responsible for natural frequency changes. It is noted that the construction of partition walls for office space in three entire levels during the spring of 2003 occurs concurrently to a significant and permanent raising of the natural frequencies (though it is shown later the magnitude of the change in frequency cannot be solely explained by the relatively small increase in stiffness expected by the addition of the partition walls).

6.2 Historical Evidence for Natural Frequency Wandering — Millikan Library

The Robert A. Millikan Library is located at the center of campus at the California Institute of Technology (see Figure 6.1). It is a nine-story reinforced concrete building with a basement and an enclosed roof (housing air conditioning equipment), completed in 1967. The library is 21.0*m* by 22.9*m* in plan, and extends 43.9*m* above grade, and 48.2*m* above basement level. Inter-story heights are all 4.27m, except between the 1st and 2nd floors, which is 4.88*m* high. The roof wall is also 4.88*m*. The structural system consists of a moment frame with large stiff reinforced concrete shear walls (30.5cm thick) on the East and West sides of the building. These shear walls provide the predominant resistance to lateral forces in the North-South direction. A 30.5*cm* thick reinforced concrete inner core adds stiffness to the building, which along with the concrete moment frame, and the bolted pre-cast concrete window/wall panels, provide the lateral stiffness in the East-West direction. The foundation system is composed of a central pad 9.75*m* wide by 1.2*m* deep, which extends across the building to the shear walls on the East and West sides. Two foundation beams (2.74*m* wide by 0.61*m* deep) run parallel to the central pad under the North and South wall respectively. A series of stepped beams transfer loads from these foundation beams to the central pad. More detailed descriptions of the structural system may be found in Kuroiwa (1967), Foutch et al. (1975), Foutch (1976), and Luco et al. (1986). The alluvium under the foundation consists of medium to dense sands mixed with gravels, and bedrock lies at a depth of about 275m. The water table appears to be at about 11*m* depth (Kuroiwa, 1967; Luco et al, 1987). Figures 6.2 and 6.3 show a North-South cross-section and a typical floor plan.

Figure 6.1: Millikan Library - View from North-East. The two dark coloured walls in the foreground comprise the 30.5*cm* thick east shear wall, which is somewhat narrower on the ground floor, due to walkway openings. The wall panels and concrete moment frame are visible on the north face

After the 1971 San Fernando earthquake, cracking and spalling of the concrete slabs located on the ground floor entry plaza was noted (Foutch and Jennings, 1978). Further, horizontal cracks along the pour line in the core shear walls between both the basement and 1st floor, and 1st and 2nd floors, have been observed in the emergency staircase in the North-South direction. Access to the East-West sides of the core shear wall is not possible. No further structural damage has been observed in the building.

In 1968, the building was instrumented with 2 permanent tri-axial Teledyne-Geotech RFT-250 accelerometers, located on the roof and basement. A 10 channel Kinemetrics CR-1 strong motion array was also installed in 1979, with channels on the basement, 6th floor, and roof. These systems have since been replaced by a 24-bit continuously recorded digital tri-axial accelerometer, the CISN (formerly TriNet) station MIK, on the 9th floor, and a 36 channel 19-bit triggered-accelerometer array run by the USGS, with a minimum

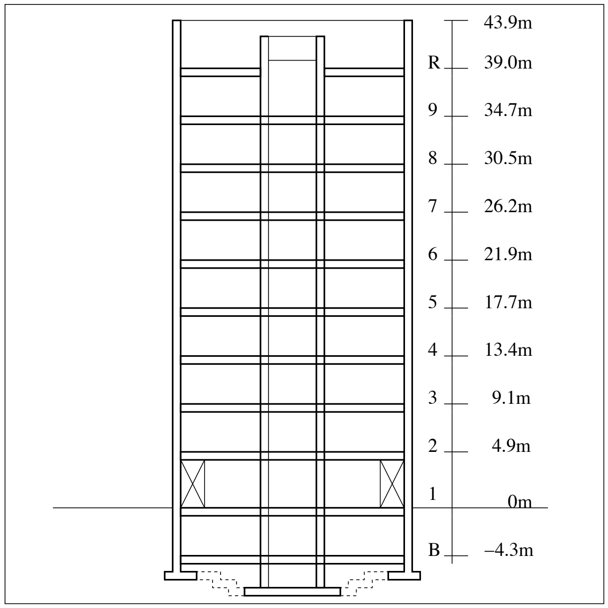

Figure 6.2: Millikan Library — North-South Section. Walkway openings on the ground floor, which cut through the shear walls, are represented by crosses.

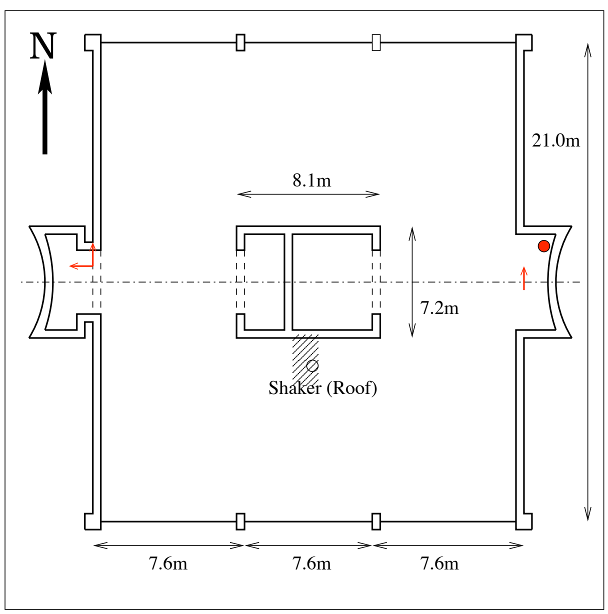

Figure 6.3: Millikan Library — Typical Plan View. The dark circle is the approximate position of CISN Station MIK on the 9th Floor, the arrows are the approximate positions and orientations of the 3 USGS channels on each floor (from 1 - Roof).

Event/Test	East - West				North - South			
	Nat Freq. *Hz*	%diff1	%diff2	mx accn *cm/s²*	Nat Freq. *Hz*	%diff1	%diff2	mx accn *cm/s²*
forced vibrations, 1967	1.45	-	-	**-**	1.90	-	-	**-**
Lytle Creek, 1970 M5.3, Δ=57km	1.30	10.3	10.3	**49**	1.88	1.1	1.1	**34**
San Fernando, 1971 M6.6, Δ=31km	1.0	31.0	31.0	**306**	1.64	13.7	13.7	**341**
forced vibrations, 1974	1.21	16.6	16.6	**-**	1.77	6.8	6.8	**-**
Whittier Narrows, 1987 M6.1, Δ=19km	1.00	31.0	17.4	**262**	1.33	30.0	24.9	**534**
forced vibrations, 1988	1.18	18.6	2.5	**-**	1.70	10.5	4.0	**-**
Sierra Madre, 1991M5.8, Δ=18km	0.92	36.6	22.0	**246**	1.39	26.8	18.2	**351**
forced vibrations, 1993	1.17	19.3	0.8	**-**	1.69	11.1	0.6	**-**
Northridge, 1994 M6.7, Δ=34km	0.94	35.2	19.7	**143**	1.33	30.0	21.3	**512**
forced vibrations, 1994	1.15	20.6	1.7	**-**	1.67	12.1	1.2	**-**
forced vibrations, 1995	1.15	20.6	0.0	**-**	1.68	11.6	-0.6	**-**
Beverly Hills, 2001 M4.2, Δ=26km	1.16	20.0	-0.9	**9.3**	1.68	11.6	0.0	**11.8**
forced vibrations, 2002 - Full Weights	1.11	23.4	3.5	**3.6**	1.64	13.7	2.4	**8.0**
- 1/2 weights	1.14	21.4	0.9	**1.9**	1.67	12.1	0.6	**4.1**
Big Bear, 2003 M5.4, Δ=119km	1.07	26.2	6.1	**14.2**	1.61	15.3	3.6	**22.6**
continuous data average - May01-Nov03	1.19				1.72			
San Simeon, 2003 M6.5, Δ=323km	1.14	21.4	0.0	**20.4**	1.54	18.9	7.8	**14.3**

Table 6.1: Natural frequencies and peak roof accelerations from selected strong motion data and forced vibration experiments. **% diff1** is the difference between the recorded frequency and that obtained in the first forced vibration tests (Kuroiwa, 1967). **% diff2** is the difference between the recorded frequency and that obtained in the most recent forced vibration test prior to the event. A complete history is presented in Tables B.1, B.2, and references for all the tests are in Table B.3. Note the 1967 entry is representative of the results from all tests from 1967 up to the 1970 Lytle Creek Earthquake — the building was already fully loaded with books.

of 3 channels on each floor. A synchronised shaker was permanently installed on the roof of the building in the early 1970's, and is still used for forced vibration testing (Hudson, 1962).

Yearly modal analysis of the structure (using temporary deployment of Kinemetrics Ranger SS-1 seismometers) during Civil Engineering classes at Caltech, as well as the triggered event data from the RFT-250 and CR-1 arrays, have provided a relatively detailed history of the evolution of the dynamic properties of the building. A summary of the fundamental natural frequencies observed during strong shaking and selected forced vibration tests is presented in Table 6.1 (for a complete list and individual references, see Appendix B). Figures 6.4 and 6.5 present graphical interpretations of Table 6.1. In Figure 6.4, the natural frequencies are plotted against date of the observation, with a clear trend towards lower natural frequencies with increasing time, with major steps occurring during large earthquakes. Figure 6.5 plots frequency versus roof acceleration amplitude, on logarithmic axes. There is a clear pattern of frequency dropping with increasing excitation amplitude. The best fitting line is a good fit to the data, though there is still a very large variance.

Kuroiwa (1967) first observed variation in the natural frequencies, measuring small amounts of frequency lowering proportional to the applied force imparted by the shaker. This has been consistently observed since then. For example, in the tests carried out in July 2002 by Bradford et al. (2004), during shaking with full weights, a E-W natural frequency of $1.11Hz$ was measured, and during shaking with only 4 side weights, the natural frequency was $1.14Hz$ - a difference of $0.03Hz$, or 2.5%. This change in weights corresponds to a factor of nearly 2 difference in the amplitude of the rooftop sinusoidal acceleration, and a factor of 2.23 change in the applied force. Similar changes were observed in the N-S fundamental frequency. Thus with weight configurations variable in some of the forced tests (and unknown in some cases), this level of variability in reporting of results should be noted. It is assumed that the forced vibration test results in Table 6.1 are made with the shaker loaded with half-full weights, and the shaded area in Figure 6.4 is a band of the likely natural frequencies reflecting the error ($\pm 0.03Hz$) arising from this uncertainty in the experimental method.

The natural frequencies from strong shaking are determined from the free resonance

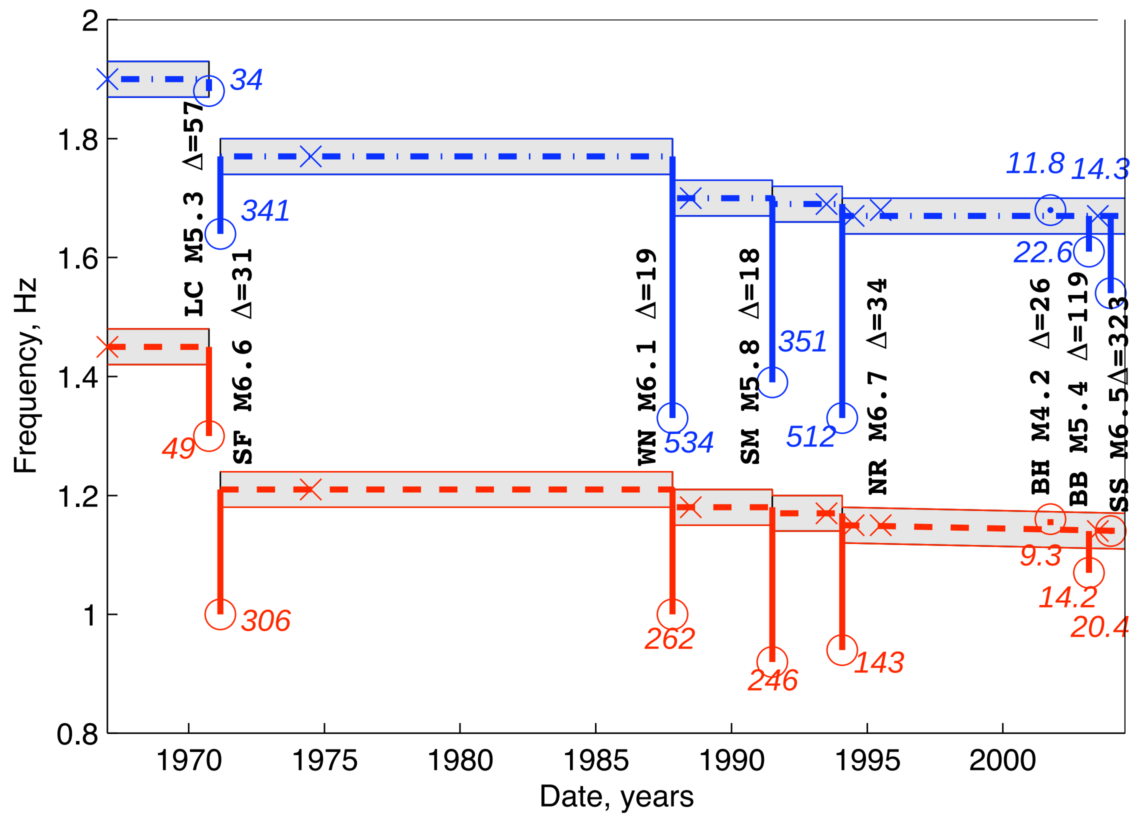

Figure 6.4: Graphical interpretation of Table 1 - Time vs. Frequency. Dashed lines are E-W natural frequencies, dashed-dotted are N-S natural frequencies, all from forced vibration testing. Shaded area is the likely region of natural frequencies taking into consideration errors in measurement, due to unknown shaker weight configuration and weather conditions for each test, and experimental error. Crosses indicate the actual time of a forced vibration measurement. Circles indicate the natural frequency estimated from the strong motion recording of the event, with the number in italics giving the peak acceleration recorded for the event (cm/s^2).

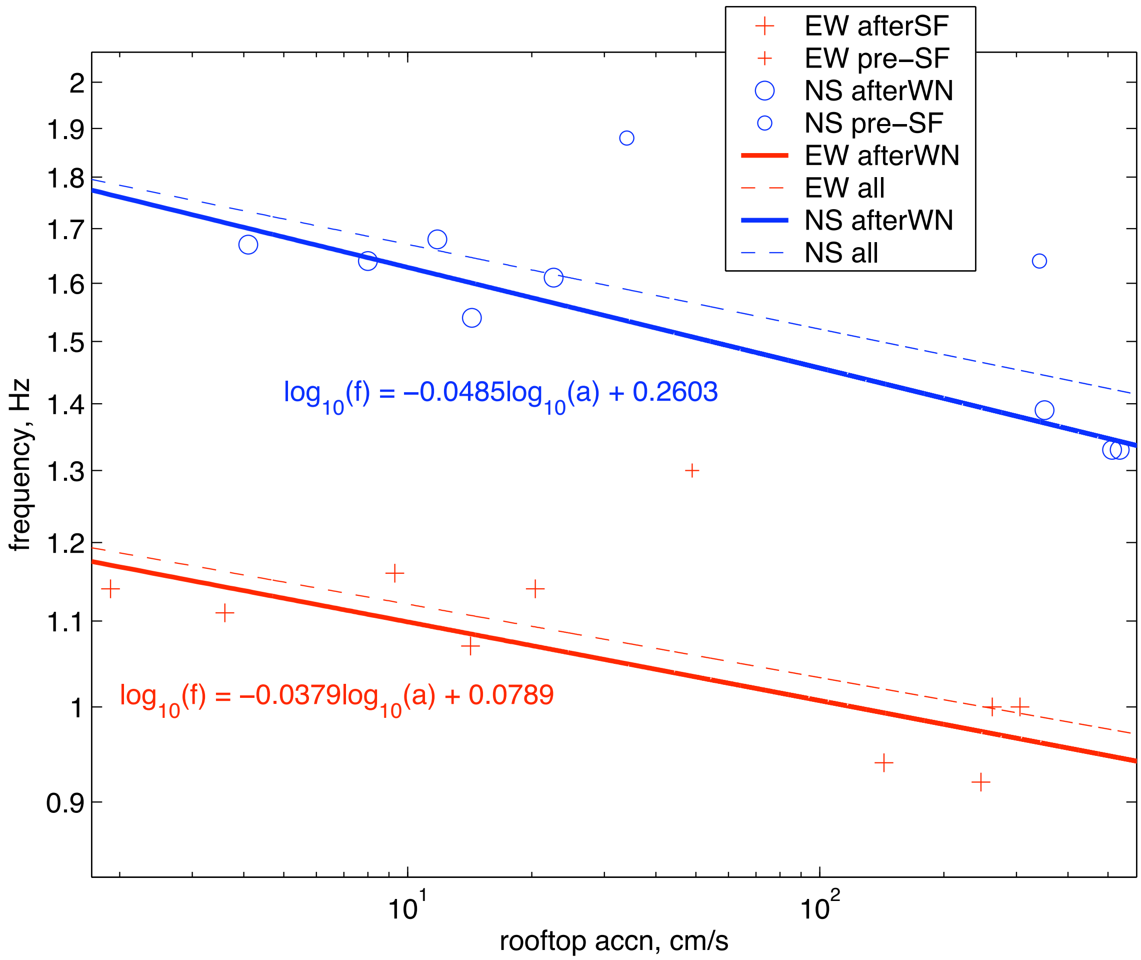

Figure 6.5: Graphical interpretation of Table 1 - Amplitude vs. Frequency, log scaling. For both E-W and N-S, the best fitting least squares solution for all the data is plotted in dashed lines. Outlying data from tests and earthquakes prior to main permanent natural frequency shift (pre- Whittier Narrows for N-S; pre- San Fernando for E-W) are removed from dataset for the solid line regressions, with labelled functional form.

of the structure (measured at the roof channels) after a large event. This is illustrated in Figure 6.6, which shows the response of the East-West Channels of the CR-1 array at Millikan to the 1987 M6.1 Whittier Narrows Mainshock (Levine et al, 1988).

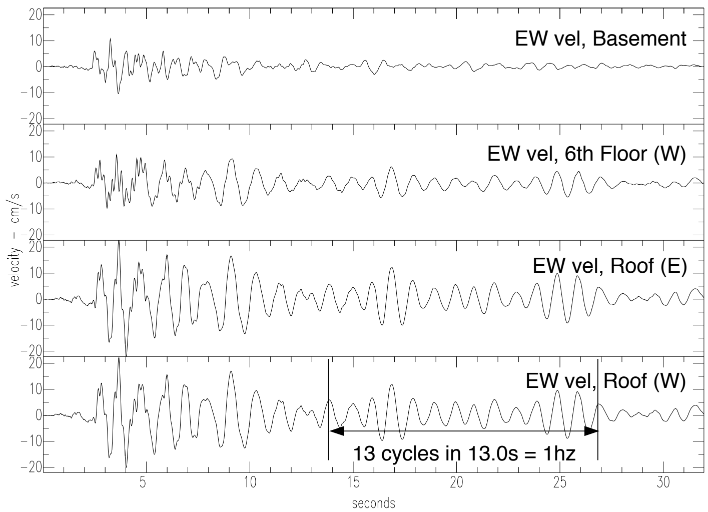

Figure 6.6: East-West components of CR-1 array in Millikan Library, recorded during the M6.1 Whittier Narrows earthquake $\Delta = 19km$ - velocity timeseries. The top trace is from the basement, the second is from the 6^{th} floor, and the last two are from the roof. The last trace includes a sample of how the fundamental frequency of the building is estimated, after the main energy (seen from the basement trace) has passed.

Table 6.1 shows the initial natural frequencies of the building at $1.45Hz$ in the E-W direction, and $1.90Hz$ in the N-S direction. For this initial test, and many subsequent tests, the higher order modes, including the first torsional frequency, are not clearly and unambiguously identified due to the poor signal to noise ratio for the recording systems of the time. (SMA-1's, CR-1's, and Ranger SS-1's all have dynamic range in the order of 3 orders of magnitude ($60dB$), compared with the $144dB$ resolution of the 24-bit instruments.) A further constraint on recovery of data at the higher modes is occupants would complain of 'motion sickness' when the library was shaken at higher frequencies during library hours.

The recorded history includes 4 large shaking events, all with roof accelerations of at least $340cm/s^2$ (over $34\%g$). Several smaller events, including the 1970 Lytle Creek earthquake, and some more recent events recorded on the digital instruments, with accelerations below $50cm/s^2$, are also included on Table 6.1 for comparison. During strong motion, the natural frequencies temporarily fall by about 20%. Surprisingly, after each strong motion event, the structural system stiffens and natural frequencies return to near pre-earthquake levels, usually with a permanent drop in frequency of less than 2.5%. Some events have led to larger permanent decrease of all subsequent forced vibration resonant frequencies. In the most extreme case, the E-W fundamental frequency dropped permanently by 16.6% in tests subsequent to the San Fernando event.

East-West Fundamental Frequency

In the E-W direction, the lateral forces are primarily resisted by the elevator core and the concrete moment frame (and possibly also from the architectural facade of stiff window frames). Table 6.1 shows that the very first significant earthquake motion (from the 1970 M5.3 Lytle Creek earthquake, $\Delta = 57km$), with comparatively small rooftop accelerations of $49cm/s^2$, resulted in a decrease of 10.3% in the natural frequency as measured in the strong motion record. A further softening occurred during the larger magnitude, closer 1971 M6.6 San Fernando event ($\Delta = 31km$, peak roof accelerations = $306cm/s^2$), with the fundamental frequency measured at about $1.0Hz$ during the strong shaking. Subsequent forced vibration tests indicate the frequency dropped permanently by 16.6%, to $1.21Hz$, from these two events. No earthquake recorded since has generated E-W motions that exceeded the velocities and accelerations of the San Fernando event. Correspondingly, subsequent natural frequencies from strong motion and forced vibration do not show any significant loss of stiffness of the structural system. The most recent E-W natural frequency recorded from forced vibrations is $1.14Hz$ (Bradford et al, 2004). The general modeshape has remained constant throughout the history (Foutch, 1976; Bradford et al, 2004).

North-South Fundamental Frequency

For the N-S direction, with the lateral resistance provided by the massive shear walls, a different pattern emerges. Very little frequency loss occurs during the Lytle Creek event - even the strong motion record shows a shortening of only 1.1%. Instead, it is the San Fernando event, with rooftop accelerations of $341cm/s^2$, that causes the first major frequency drop; natural frequencies from forced vibrations fell from $1.9Hz$ to $1.77Hz$ after the event. Modeshapes before and after San Fernando show major differences, before the earthquake, less than 3% of the peak displacement at the roof is attributed to basement rocking, yet after, and in subsequent tests, approximately 30% of the roof motion is due to basement rocking (Jennings and Kuroiwa, 1968; Foutch, 1976; Bradford et al, 2004). Another major decrease occurs during the 1987 M6.1 Whittier Narrows event ($\Delta = 19km$), where the highest rooftop accelerations ($534cm/s^2$) were recorded during the shaking. Figure 6.4 shows that this event caused the largest intra-event frequency drop (nearly 25%), with a 4% permanent decrease in forced frequencies. Subsequent natural frequency measurements from forced vibration tests are relatively constant, and no further softening beyond the $1.33Hz$ recorded in Whittier Narrows occurs during strong motions (including the Northridge earthquake). The most recent forced N-S natural frequency is $1.67Hz$ (Bradford et al, 2004).

East-West 2^{nd} Mode Frequency

At construction, the 2^{nd} E-W mode frequency was determined as $6.2Hz$ (Kuroiwa, 1967). During San Fernando, the frequency dropped to $\sim 4.95Hz$ (McVerry, 1980; Beck and Chan, 1995). Investigations subsequent to this earthquake have indicated the 2^{nd} mode varies from $4.17Hz$ (Beck and Chan, 1995) to $5.35Hz$ (Teledyne-Geotech-West, 1972). The most recent measured forced E-W 2^{nd} modal frequency is $4.93Hz$ (Bradford et al, 2004).

Response to Small Earthquakes

Table 6.1 also contains fundamental frequencies determined from shaking due to the small M4.2 Beverly Hills event ($\Delta = 26km$) in September 2001. Even though measured accelerations from the event are about double the accelerations from the sinusoidally excited forced vibration tests, the measured fundamental frequencies are higher than those from forced testing. This may be attributed to changes in the ambient pre-earthquake natural frequency due to climatic changes - and will be discussed in detail later.

The February 2003 M5.4 Big Bear event ($\Delta = 119km$) produced accelerations almost double those from the M4.2 Beverly Hills event, and yet it had a more significant effect on the fundamental frequencies — the drop in frequency from Big Bear is much greater than double the drop observed in Beverly Hills. This suggests that the relationship between fundamental frequency and acceleration is non-linear. Further, it is observed that the fundamental frequency during the Big Bear event drops by 6.1% in the E-W direction, and only 3.6% in the N-S direction, even though the N-S accelerations are larger. This indicates that the E-W direction is more susceptible to softening under small excitations, and that larger motions are required to start significant softening in the N-S direction (the ambient data will corroborate this observation). The response of the library to this earthquake is studied in more detail later. Figure 6.5 indicates there is in general a linear relationship between the logarithm of the acceleration amplitude and logarithm of the frequency, though the scatter of the data is large, and, at least for the small amplitudes, may be due to the ambient variations in natural frequencies.

6.3 The Current System of Instrumentation at Caltech

There are currently 5 buildings on the Caltech campus with real-time telemetry of high-dynamic-range digital instrumentation. These are the Millikan Library, the Broad Center for the Biological Sciences, the USGS Building at 525 S. Wilson Ave, the Robinson Building and the Athenaeum. A dense array at Millikan Library is comprised of triggered digital accelerometers with dial-up data retrieval.

The Caltech Civil Engineering Department operated an older network of analog film-recording SMA-1's at a number of sites on and around the campus, as well as a 12-channel CR-1 at Millikan Library, which had been operational on campus since the 1970's. However, this network has not been maintained since the mid-1990's, and is currently not operational.

The digital stations currently operating at Caltech are described in the following subsections

6.3.1 Millikan Library (MIK, USGS-Caltech Array)

In January 1998 the USGS and Caltech Civil Engineering Department installed a 36 Channel dense network of FBA-11 accelerometers recording triggered event data on 2 19-bit Mt. Whitney dataloggers with dial-up data retrieval. A tri-axial EpiSensor accelerometer was also installed on the 9th floor of the structure and has been continuously transmitting 24-bit data since February 2001 to the Southern California Earthquake Data Center (SCEDC), as Station MIK in the California Integrated Seismic Network (CISN).

This improved sensor configuration prompted a detailed forced dynamic analysis (using the existing shaker located on the roof), which was performed in the Summer of 2002, (Bradford et al, 2004). The results of this study are summarised in Table 6.2. At the time of the tests, the approximate first mode frequencies during forced vibration (1/2 weights) are $1.14 Hz$ for the East-West direction, $1.67 Hz$ for the North-South direction, and $2.38 Hz$ for the torsional mode.

	Millikan Library [*Hz*]			**Broad Center** [*Hz*]	
Orientation	1^{st} **Mode**	2^{nd} **Mode**	3^{rd} **Mode**	1^{st} **Mode**	2^{nd} **Mode**
East-West	1.14 [*1.19*]	4.93	7.83	2.67	3.01
North-South	1.67 [*1.72*]	7.22	?	2.43	2.81
Torsional	2.38 [*2.46*]	6.57	?	3.65	?

Table 6.2: Natural frequencies for the Millikan Library and the Broad Center. Millikan Library frequencies are from forced vibration tests, Summer 2002 (Bradford et al, 2004). For the 3 fundamental frequencies, in parentheses are the 2-year average frequencies from continuous ambient MIK data. Broad Center results are from the ambient vibration data from 14-days of continuous data during February 2003, and are preliminary (in the absence of a forced vibration modal analysis of the structure).

6.3.2 Broad Center (CBC)

The Broad Center is a 3-story structure with an irregular floor plan and 2 deep basements (see Figs 6.7 and 6.8). It was completed in the Summer of 2002, and has been instrumented since February 2003. The basements are enclosed by stiff shear walls, and the steel superstructure is braced with stiff unbonded braces in both the North-South and East-West directions.

Figure 6.7: Broad Center - View from South-West.

Figure 6.8: Broad Center - View from North-West. Structural core of the unbonded-brace frame is located below the parapet wall visible on the roof (Figure 6.9 contains a plan view).

The building houses a 24-bit CISN station, recording 8 channels of EpiSensor accelerometer data. Three tri-axial instruments are installed, all on the plan of the unbonded braced frame-line that is the structural core of the building. Two are located near the N-W intersection of the frame-line, one on the 1st floor, with the other on the roof. The final accelerometer, which only has its horizontal channels logged (the datalogger supports only 8 channels of data), is near the S-E intersection of the frame-line. All 8 channels comprise CISN station CBC. The instrument layout is illustrated by the schematic in Figure 6.9.

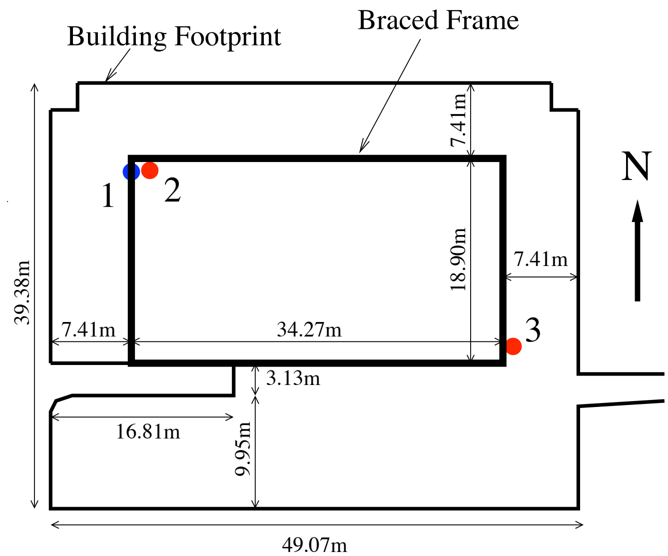

Figure 6.9: Broad Center — Schematic plan view showing placement of strong motion sensors. 1 is on First floor; 2 and 3 are located on the roof.

In the absence of a forced vibration modal analysis for the building, the natural frequencies were investigated using the CBC ambient data alone. The FFT amplitude spectra from 14 1-day recordings of ambient vibrations were stacked together, with obvious spectral peaks emerging. Table 6.2 presents the resonant frequencies determined by this analysis.Figure 6.10 shows the FFT's from each of the channels, with these selected frequencies highlighted. In both the E-W and N-S directions, 2 modal frequencies very close in frequency to each other are observed. A torsional mode is at $3.65Hz$, clearly observed with out-of phase motions in the time-domain from both the E-W and N-S roof channels located in the N-W and S-E corners of the roof. A mode shape analysis using CBC data alone is not possible as there is instrumentation at only 2 levels in the building. As the lowest E-W and N-S frequencies are relatively stronger than the higher E-W and N-S frequencies in the 1st floor, but much weaker at the roof, it is inferred that the lower frequencies likely correspond to a translational and rocking mode arising from soil-structure interaction, and the higher frequencies correspond to a structural shearing mode for the superstructure, which has large displacements at the roof, and small displacements at the 1st floor. Unfortunately, analysis of the displacement data from each channel, bandpassed around each natural frequency, does not fully support these conclusions. Further, it is very rare to observe individual natural frequencies clustered so close together in a structure. Potentially there could be a local effect in the building not yet appreciated. Ideally, further instrumentation and a forced vibration test are needed to confirm the dynamic properties of the structure.

6.3.3 525 S. Wilson Ave — USGS Office (GSA)

GSA is a 24-bit CISN station with a tri-axial EpiSensor accelerometer located in the basement of the 2-story wood-frame house (used as USGS Pasadena Offices). GSA data is currently used as a reference station for data from the Millikan Library and Broad Center. The station, operating since July 2000, is approximately 150m due West of the Millikan Library, and about 200m SSW of the Broad Center.

6.3.4 Robinson Building (CRP)

CRP is a 24-bit CISN station, located about 18m below grade, in the un-used Solar Telescope pit of the Robinson Building. It is currently used as a test station, and so can have a variety of instruments, though it always has one high-gain broadband (STS-2 or CMG-1) and one strong motion (EpiSensor or VSE-355G2) instrument deployed. It is the only station on campus with a high-gain digital instrument permanently deployed. It has been operational since March 2003, and is about 75m SW of Millikan Library.

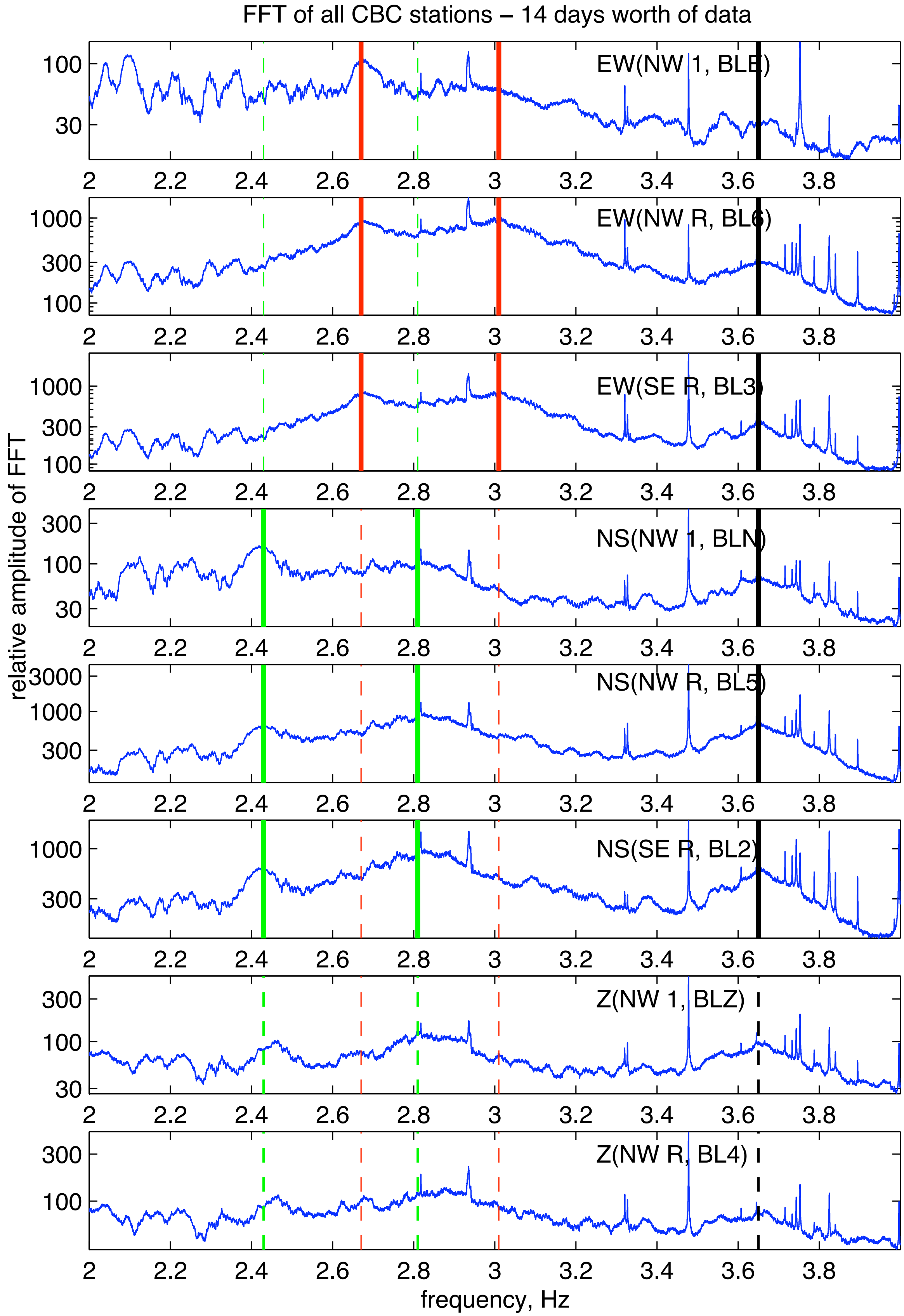

Figure 6.10: Broad Center — Stacked FFT data from 14days in February. Suspected natural frequencies shown by vertical bars: red - EW (2.67, 3.01Hz); green - NS (2.43, 2.81Hz), black - torsional (3.65Hz).

6.3.5 The Athenaeum (CAC)

CISN station CAC is a 19-bit K-2 datalogger with a tri-axial accelerometer deployed at the Athenaeum. Located in the basement, CAC occupies the same site as the old analog Athenaeum/Caltech station that has recorded earthquakes since the 1960's. Data is continuously telemetered to the CISN/SCEDC, but as the information is only 19-bit, only events that trigger on the network are permanently stored in the SCEDC.

Continuous and triggered data from these (and all other) CISN stations may be obtained from www.scecdc.scec.org/stp.html. Triggered data from some of the events recorded by the USGS-Caltech array on Millikan Library is available at nsmp.wr.usgs.gov/data.html.

6.4 Analysis of the Continuous Data Streams

As discussed in the previous section, two buildings on the Caltech campus, Millikan Library and the Broad Center, have continuous recording of data in the SCEDC from instruments located on the upper floors of a building. Thus these data streams can be used to analyse the evolution of each building's natural frequencies over the life of these stations, and at other interesting length scales. The natural frequency changes are correlated with weather data from the JPL Weather Station. This is the nearest digital continuously-monitored weather station, and it is located $8.5km$ North of the Caltech buildings at the Jet Propulsion Lab. Data is available from the start of continuous data storage from MIK, up to the end of November, 2003. This includes 2.5 years of data for MIK, and 10-months for CBC, which only started recording in mid-February 2003.

The JPL weather station logs data every second; the channels used for comparison are rainfall (cumulatively measured per day, mm), wind gusts (m/s), and temperature (^{o} Celsius). Subsequent plots present only total rainfall, maximum wind gusts and the maximum and minimum temperatures.

6.4.1 Entire Station Duration — MIK and CBC

Figure 6.11 is a spectrogram plot for the entire history of the station MIK, alongside JPL weather data. The three individual spectrogram sub-plots are centred about the three fundamental frequencies. Figure 6.12 plots the same data without scaling the peak of each 1 hour spectrogram slice to unity. Figure 6.13 is a similar spectrogram for the history of station CBC, and Figure 6.14 is the same without scaling of each slice. As the natural frequencies at CBC are not well-determined, individual spectrogram sub-plots are presented for each of the E-W and N-S channels, over a wide range of frequencies which encompass the observed spectral peaks.

Spectrograms are ideal for illustrating the evolution of the magnitude and frequency of any particular resonance, or energy over time. The spectrograms are colour plots with time on the x-axis, and frequency on the y-axis. At each point in the plot, the colour represents the intensity of the acceleration at MIK for the particular time and frequency. Each spectrogram is made by dividing the acceleration timeseries up into lengths of time (a slice) and taking the FFT of this time window. The magnitude of the FFT is then represented by a colour contour along the y-axis at the time on the x-axis to which the FFT corresponds (the mid-point slice time). Plotting this for each slice leads to the composite spectrogram. In Figures 6.11–6.14, the FFT length is 1-hour long, and there is no time overlap between slices. Each FFT has also been first smoothed over a frequency of $0.002Hz$ and then decimated to a sampling frequency of about $0.001Hz$. In these Figures, the acceleration amplitude scaling is linear for both MIK and CBC, with upper and lower bounds arbitrarily set to prevent unusual highs, such as the 22 Feb 2003 Big Bear earthquake, from swamping the colourbar.

As the three fundamental frequencies of Millikan Library are well separated and of large magnitude, the hourly peak in the FFT can be traced over time, as seen in Figure 6.15. Here the average of all the peaks is determined, and the deviation from this average is plotted. The daily average of the FFT peak is plotted as a thick line, with the hourly FFT peak as a thin line. The timing of small earthquake excitations, and forced vibration testing of the structure are highlighted by vertical bars. These are the source of the obvious large deviations from the mean.

Figure 6.15 shows considerable variation in natural frequencies over the last 2 years. In particular notice the sensitivity of the fundamental E-W and torsional modes to rainfall, as evidenced by the large shifts during the winter months, when storms with several days of rainfall are a regular occurrence in Southern California. These rain events are infrequent during the summer months. The N-S mode does not seem to be as sensitive to the rainfall, and in general, it has smaller short-term deviations than the E-W and torsional modes. Also note a steady and unusual rise in the three fundamental frequencies during the spring of 2003, from April to July 2003. This occurs at the same time as a change in usage of 3 mid-level floors of the Library (3^{rd}, 4^{th} and 5^{th}), from housing library volumes to providing office space. The books were removed during the summer of 2002, with little apparent change in the natural frequencies. However, the construction of partition walls for the new offices in the spring/summer of 2004, coincides with the gradual rise of about 4% in E-W natural frequency. The rise is less pronounced in the N-S and torsional modes. The natural frequency of a building is proportional to the square root of its stiffness, so an increase of 4% in natural frequency is equivalent to an increase of 8% in stiffness. It does not seem plausible that such a large increase in stiffness can be attributed alone to the installation of partition walls (which only rise up to the false ceiling).

Discounting this recent lengthening trend, from the plots the following maximum variation for the daily average over the last 2 years are observed:

	E-W	N-S	Tors.
min	1.155Hz	1.71Hz	2.44Hz
max	1.215Hz	1.74Hz	2.55Hz
variation	0.06Hz	0.03Hz	0.10Hz
	5.1%	1.7%	4.4%

Figure 6.13 presents the first 10-months of data recorded at CBC. Table 6.2 indicates the suspected natural frequencies of the building. As these modes have not been well determined from a forced vibration test, a range in frequencies from $2.4Hz$ to $4.1Hz$ is presented for the N-S and E-W channels separately. There is significant machine noise,

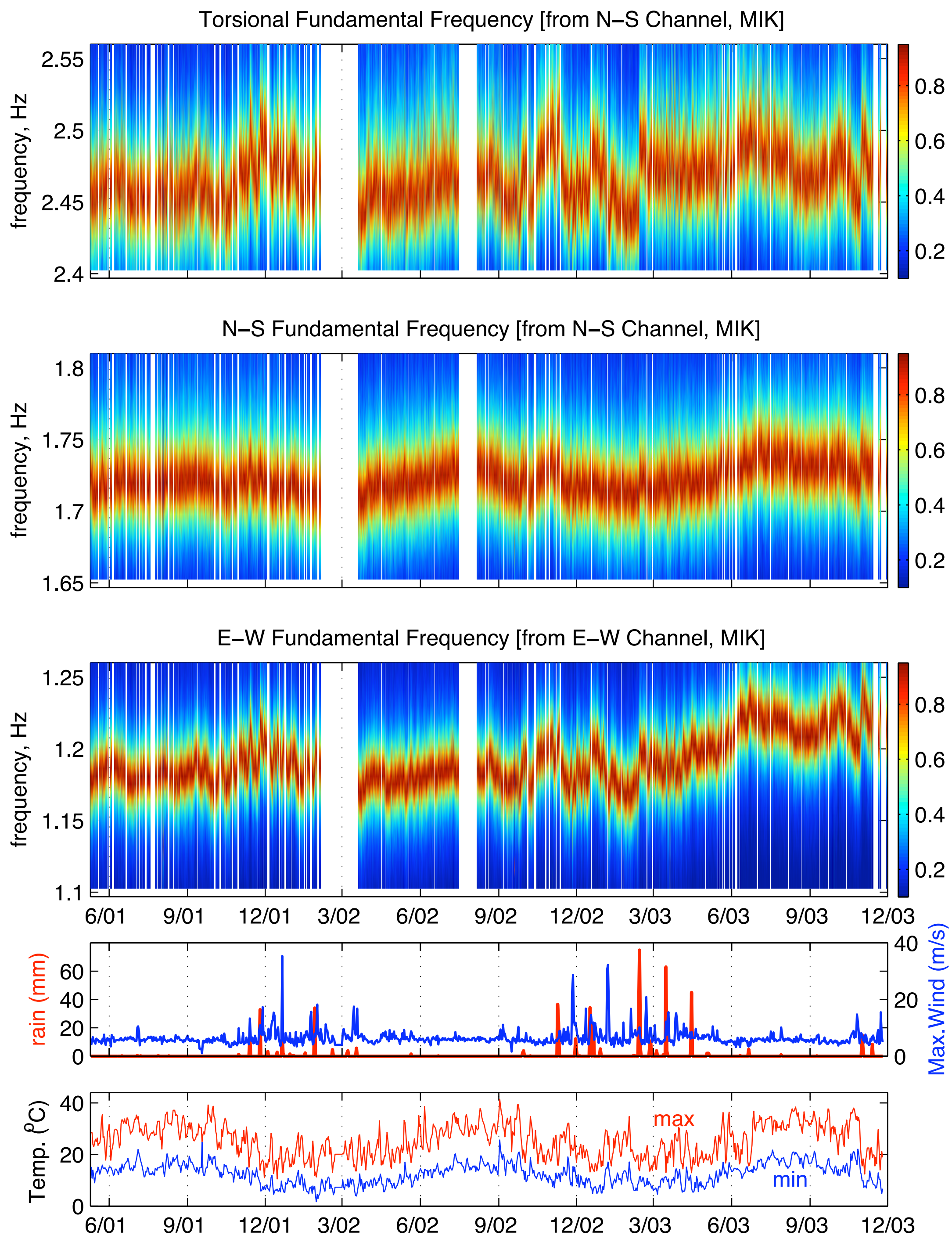

Figure 6.11: Spectrogram of natural frequencies as observed at MIK, for current station lifetime (May2001 - Nov2003). Spectrogram composed of 1 hour time windows, each scaled so max. is 1, and plotted with linear colourbar. Weather data is from JPL weather station ($\Delta = 8.5km$). Vertical breaks in data due to days with data glitches or no recorded data. Tick marks on x-axis correspond to 1^{st} of the month labelled underneath. The peaks in natural frequencies are observed to wander over the course of the 2.5 years. No longterm correlation with temperature is observed, though rain causes temporary lengthening of natural frequency.

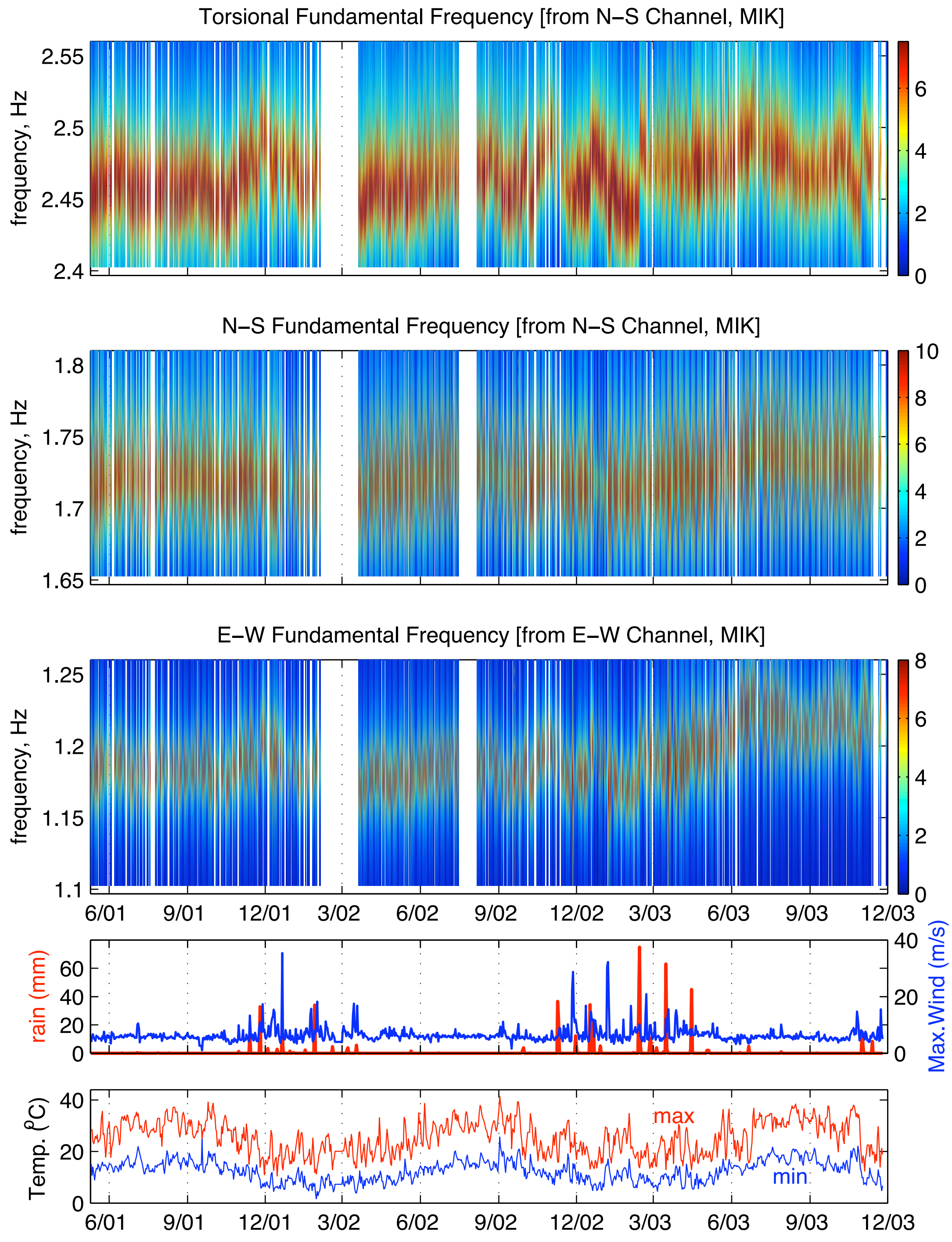

Figure 6.12: As Figure 6.11, no scaling of each spectrogram slice, linear colourbar

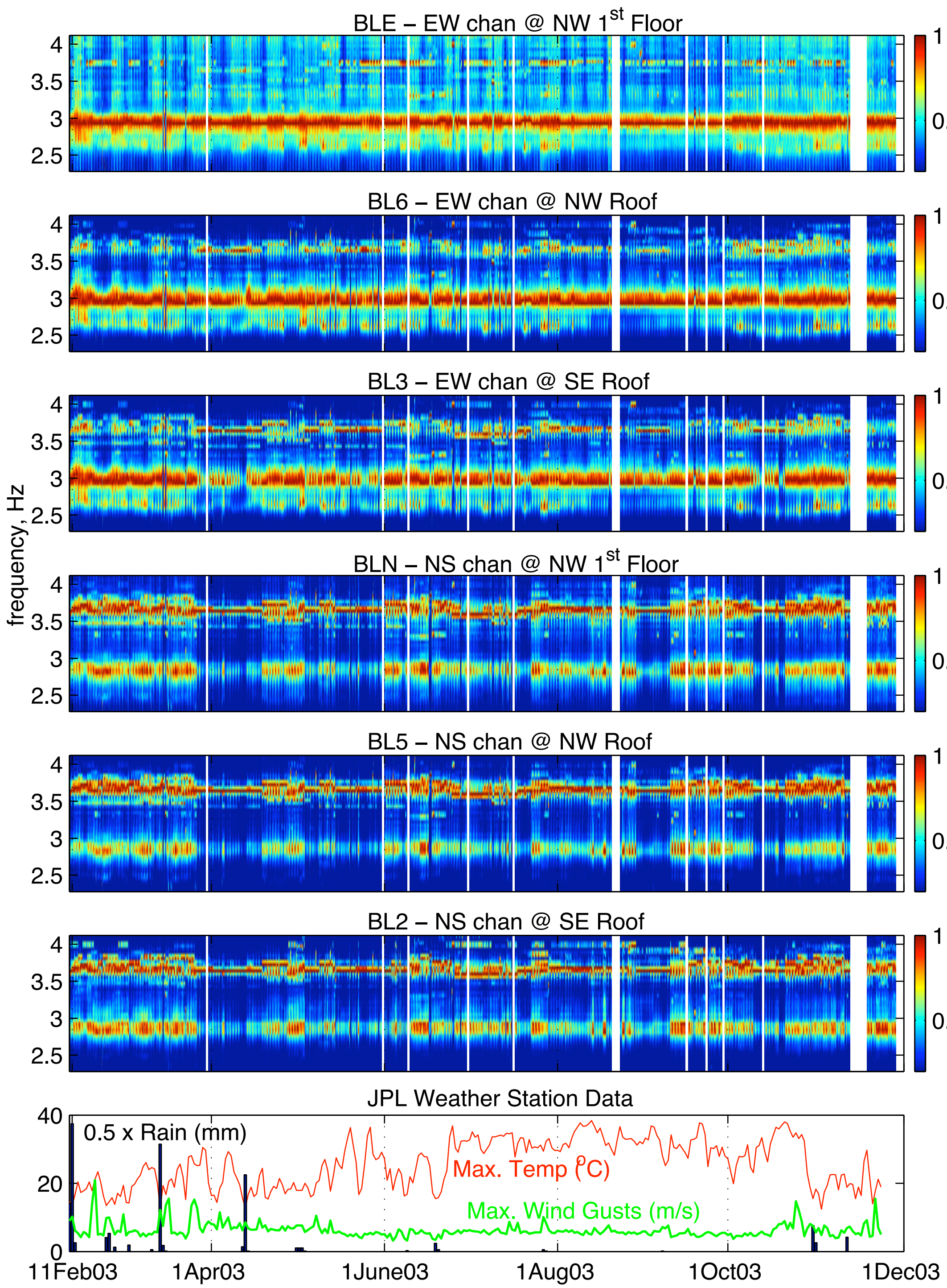

Figure 6.13: Spectrogram of all 6 horizontal channels at Station CBC, the Broad Center, for current lifetime of Station (Feb2003 - Nov2003). 1 hour spectrogram windows, no scaling, linear colourbar. Sharp red horizontal lines are due to machine noise in the building. Natural frequencies are represented by the broad peaks, near $2.6Hz$, $3.0Hz$ and $3.6Hz$, for the E-W channels, and near $2.4Hz$, $2.8Hz$ and $3.6Hz$ for the N-S channels. Notice the $7day$ noise cycle with relative quiet on the weekends.

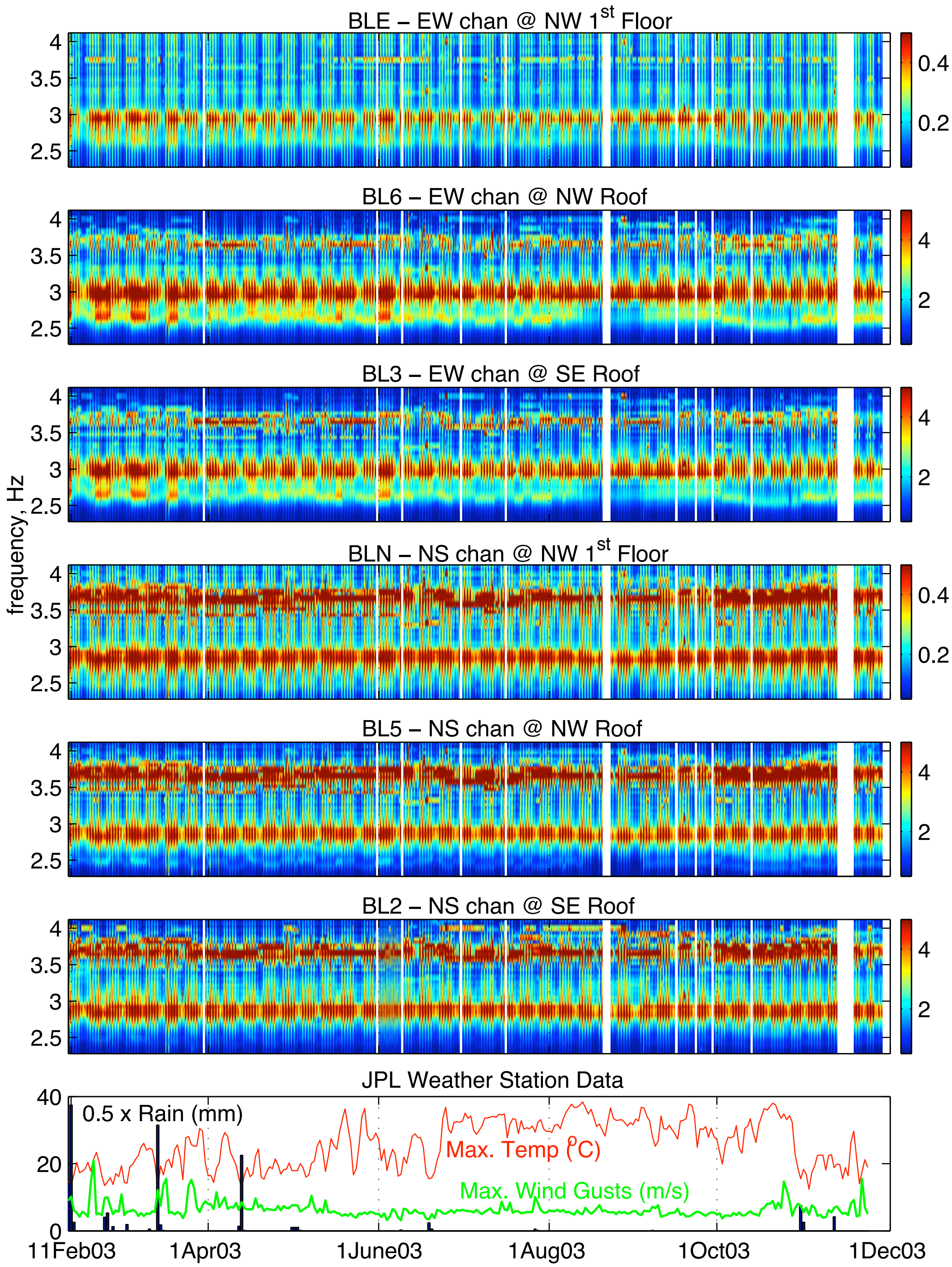

Figure 6.14: As Figure 6.13, no scaling of each spectrogram slice, linear colourbar

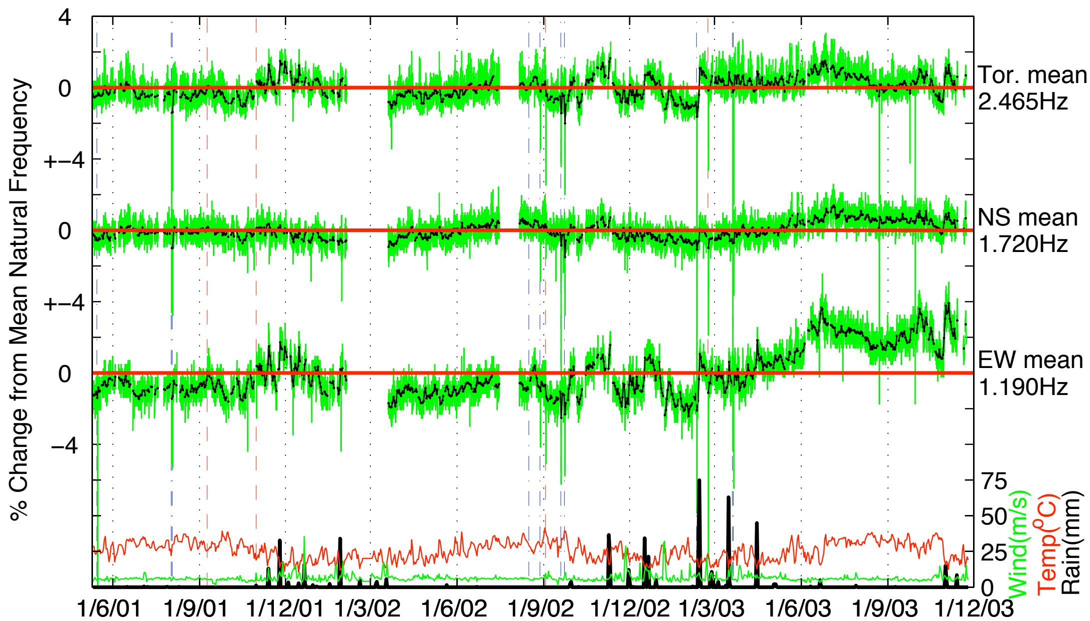

Figure 6.15: Deviation from the mean natural frequency for the 3 fundamental frequencies as recorded at MIK for station lifetime (May2001 - Nov2003). Fundamental frequencies for each hourly FFT are picked from the peaks in Figure 6.11, then the deviation from the average is determined. From the top down, the torsional, N-S and E-W frequencies are plotted. Hourly peak is shown in light thin line for each frequency, the thick black line tracks the daily average. The thick horizontal line is the average frequency. Rain, wind and temperature are plotted at the bottom. Vertical dashed-dot and dashed lines indicate days with forced vibration shaking of the library, and earthquakes with motions exceeding $2.5cm/s^2$ at station MIK, respectively. These are responsible for the large deviations from the mean. [Earthquakes: 9/9/01:M4.2 Beverly Hills, $7cm/s^2$; 30/10/01:M5.1 Anza, $2.8cm/s^2$; 3/9/02:M4.8 Yorba Linda, $5cm/s^2$; 22/2/03 M5.4 Big Bear, $18cm/s^2$]. Note: forced vibration with full weights generates $8cm/s^2$ at N-S fundamental mode.

characterised by the heavy horizontal red and yellow lines, near the natural frequencies at $3.65Hz$ (torsional), $2.81Hz$ (N-S) and $3.01Hz$ (E-W). It appears these frequencies are being driven by the machine noise, and so subtle shifts in their frequency over time would not be easy to interpret if it is indeed occurring.

The two lowest N-S and E-W frequencies, near $2.43Hz$ and $2.67Hz$ respectively, are not near any machine noise, and do seem to exhibit temporal changes similar to that seen in Millikan Library. Figure 6.16 presents a close-up of these lower frequencies for all the horizontal channels. Figure 6.17 presents the same data with no scaling of the colourbar. Large variations in signal strength over the time period are observed, with significant variation in the natural frequencies themselves. For the first 6-months, there is periodic variation, with period of the order of 2 weeks. After this, the predominant period of variation is much longer, on the order of months. The lowest E-W frequency seems to vary from $2.55Hz$ in mid October to $2.72Hz$ in early February, a variation of $\sim 6.5\%$. The lowest N-S frequency is of smaller amplitude to the lowest E-W mode, and thus is harder to observe above the ambient noise, and is only clearly visible on the N-W roof channel, BL5. It varies from $\sim 2.40Hz$ in mid October and $\sim 2.52Hz$ in early May, a variation of $\sim 4.9\%$. This N-S mode appears to disappear in late August, and in mid October drops to $2.4Hz$ for a number of weeks, coinciding with a large drop in the E-W lowest mode. Rainstorms, such as in early February and early November, clearly raise these resonant frequencies in a similar manner to what is observed in Millikan Library. The spectrograms also have a strong daily and weekly cycle, as much of the machinery is turned off during the nights and weekends.

6.4.2 Winter Storms — MIK

The temporal variations at MIK (Figure 6.15) can be partially explained by correlation with the rainfall data from the nearby JPL Weather Station. Figure 6.18 is a similar plot to Figure 6.15, focusing on the Winter of 2002/2003. In this 7-month period, heavy winds and rains were recorded. Each rainfall event prompts an immediate rise in the natural frequencies, which is largest in the E-W and torsional modes. After the storm, in the absence of other unusual excitation (such as windstorm, forced vibration test or earthquake), a gradual

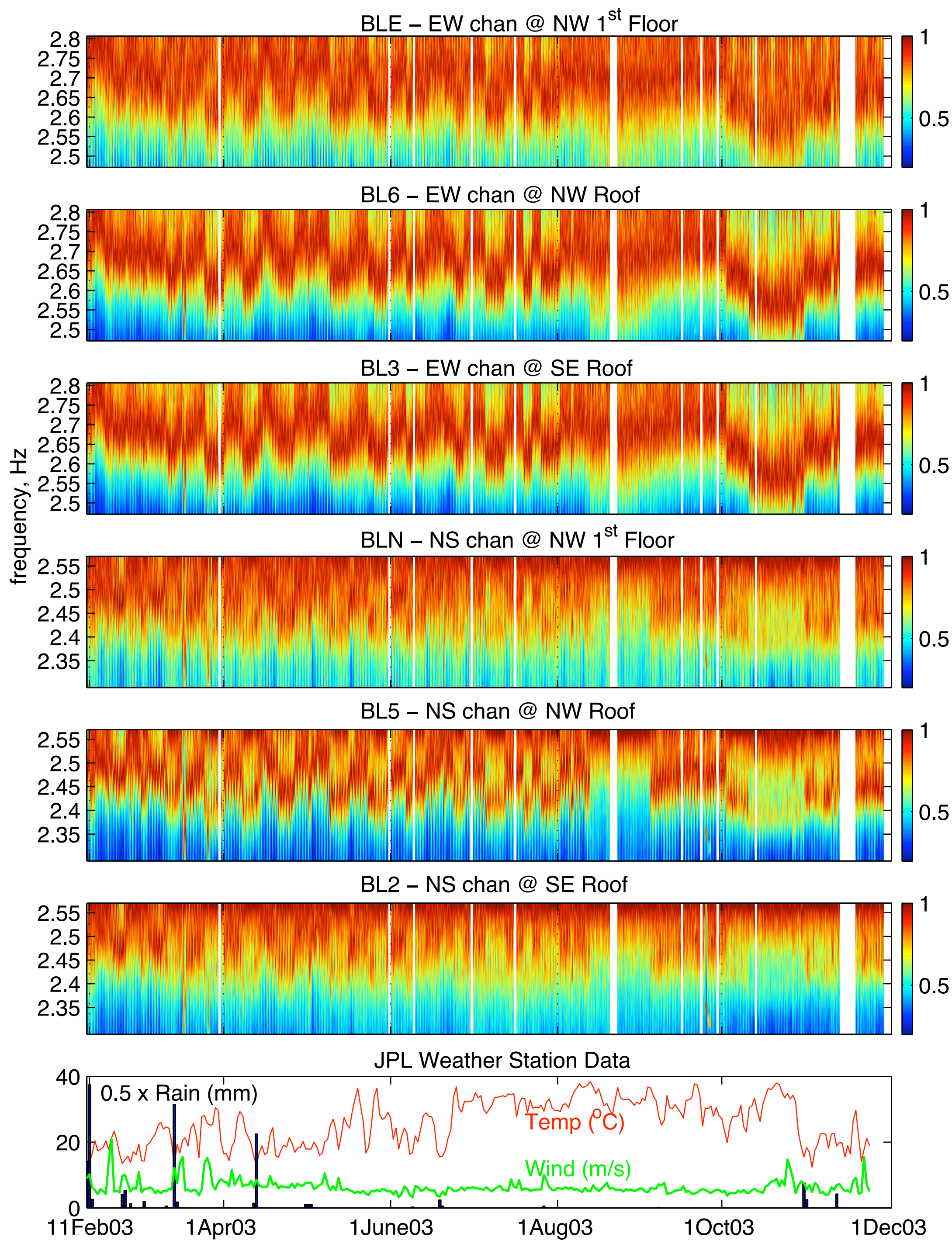

Figure 6.16: Spectrogram of fundamental frequencies for Broad Center, for current lifetime of Station CBC (Feb2003 - Nov2003). 1 hour window of spectrograms, scaled by max. value, linear colourbar. E-W channels centred around 2.67Hz, and N-S channels around 2.43Hz, the natural frequencies determined from stacking of 14-days of day long FFT's (Table 6.2). Note the rainfall seems to coincide with sudden rises in frequency, as observed at MIK.

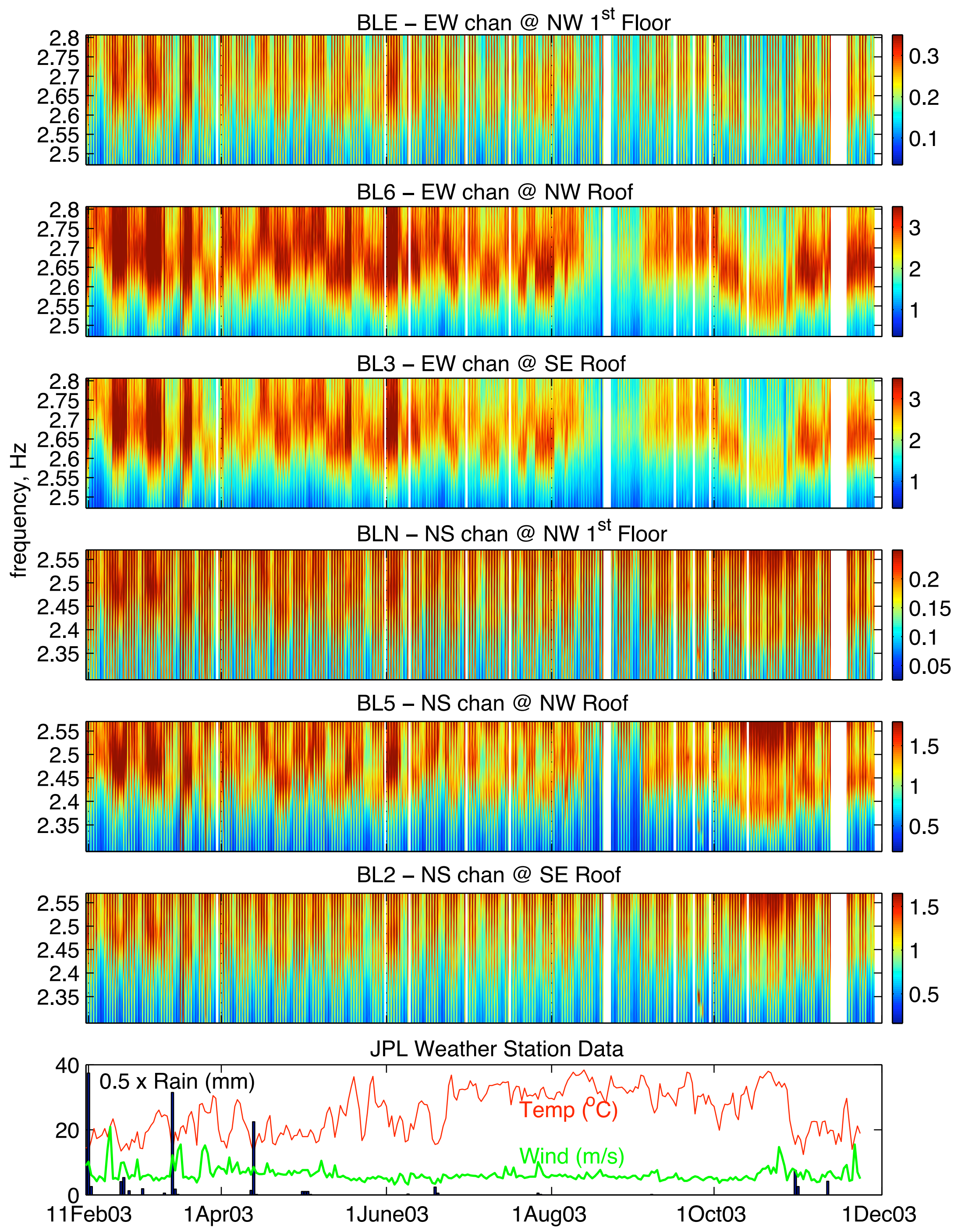

Figure 6.17: As Figure6.16, no scaling of spectrogram, linear colourbar.

recovery (on the order of about a week) of the frequencies to near the pre-rainfall levels is observed.

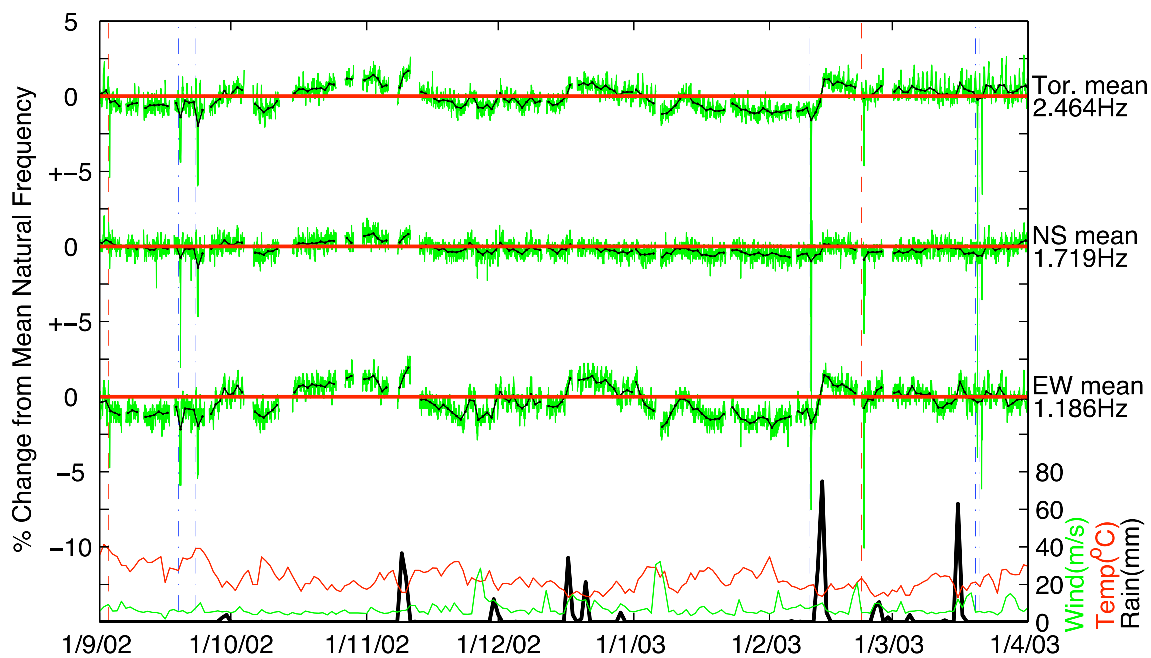

Figure 6.18: As Figure 6.15, with duration from September 2002 to March 2003, showing Millikan Library response to the storms recorded during the Winter season.

Figure 6.19 is a close-up of the period including the most severe storm since the installation of MIK, when over 100*mm* of rain fell over 2-days in early February 2003. This event caused a rapid and immediate rise of about 3% for the E-W and torsional natural frequencies, with a slow decay towards pre-rainfall levels over a 10 day period.

Figures 6.20 and 6.21 show a spectrogram of the E-W fundamental and 2^{nd} mode frequencies over the same time period, February 2003. An obvious rise in frequency of $\sim 3\%$ is observed in the 2^{nd} mode, with a similar return towards pre-rain frequencies as shown by the fundamental mode. The same trend is seen in Figures 6.22 and 6.23 during the rain events for the period of October - November 2003.

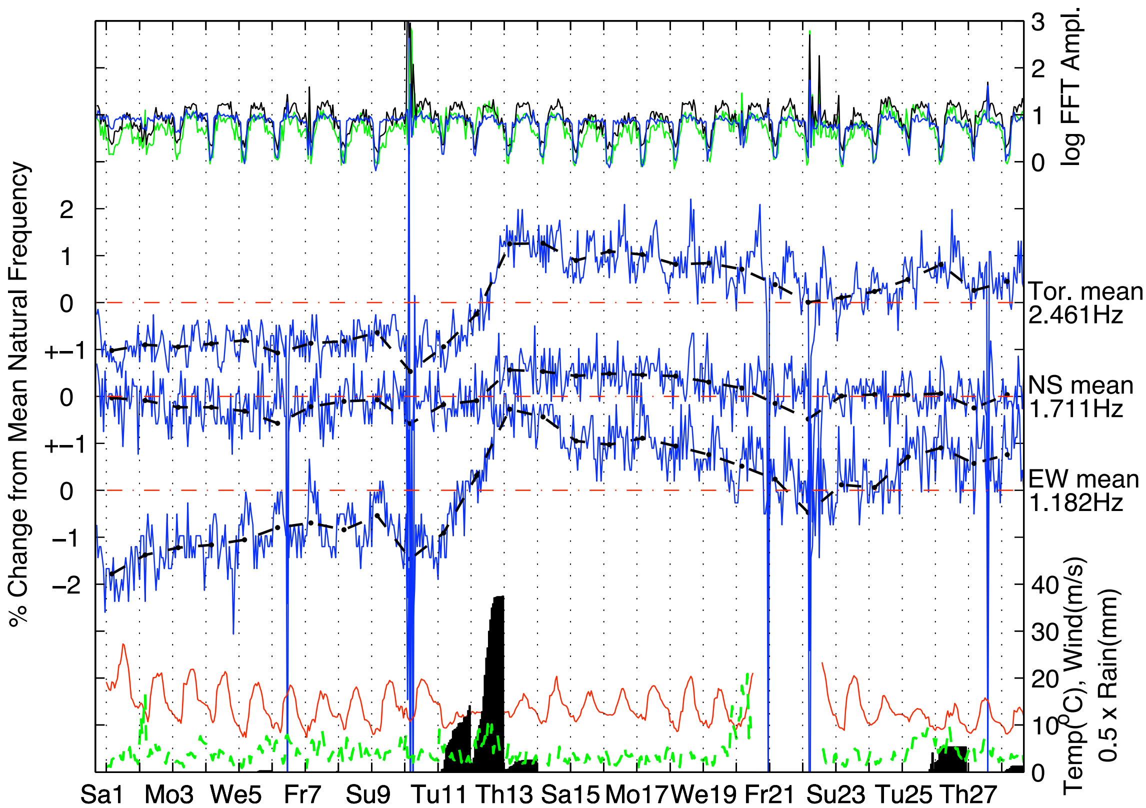

Figure 6.19: Deviation from the mean for the 3 natural frequencies of Millikan Library, for February 2003, including the major rainstorm from 11-12 February. In the centre of the plot, for each of the 3 natural frequencies, the horizontal dashed lines are the monthly average, the dashed-dotted lines are the daily average % deviation from this mean, and the solid light lines are the hourly % deviation from mean. At the bottom of the figure, the black bar data is the cumulative hourly rainfall (re-zeros at midnight). The solid line is the maximum hourly temperature, and the dashed line is the wind gust. On the top of the figure is the amplitude of each hourly FFT peak. The rainfall coincides with a very sharp rise in natural frequencies in the E-W and torsional modes, with slow return towards pre-rainfall levels afterwards. Dashed vertical lines represent the start of each new day (12AM PST). Frequency spikes are due to instrument glitches (6, 21, 27 February), vibration testing (10 February) and the Big Bear earthquake (22 February). FFT peaks fall at night, and on weekends. No major increase in excitation amplitude occurs during rainfall events not associated with high winds.

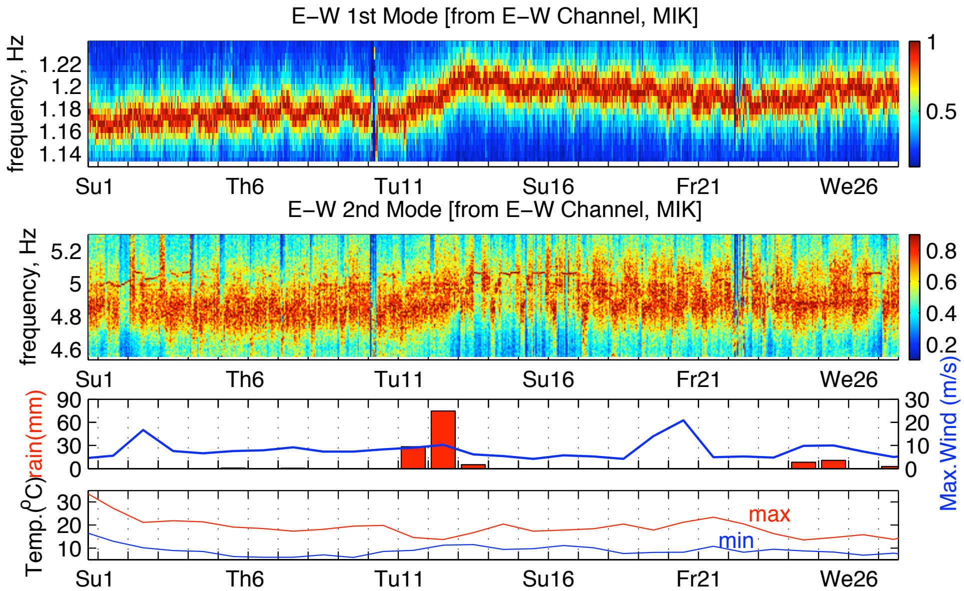

Figure 6.20: Spectrogram of Fundamental and 2^{nd} mode frequencies for E-W mode during February 2003, a time of heavy rainfall. 1 hour spectrogram windows, scaled by the maximum value, linear colourbar. JPL weather on bottom. Note correlation between rises in both natural frequencies and heavy rainfall.

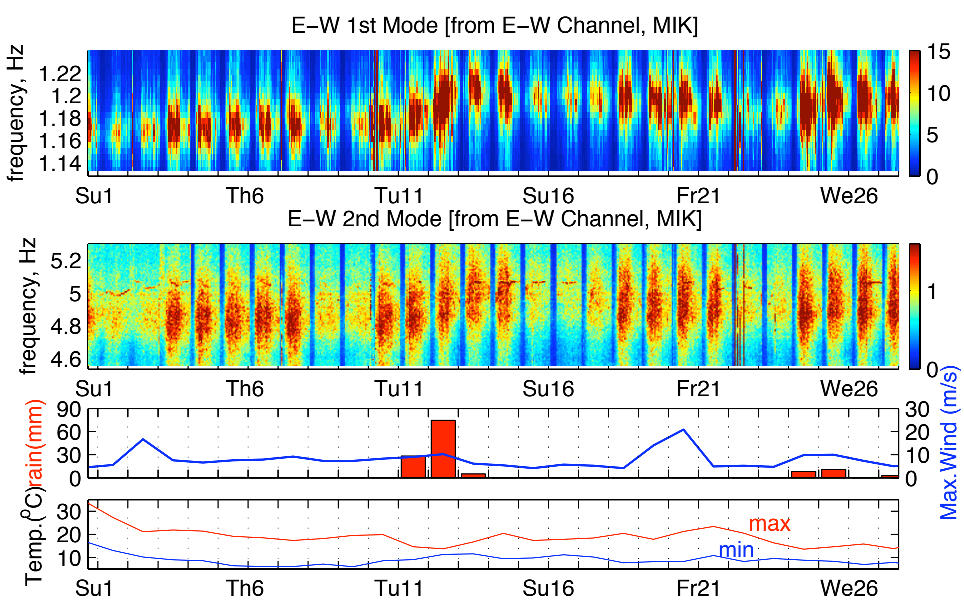

Figure 6.21: As Figure 6.20, with no scaling of each spectrogram, so variations of intensity of each frequency are apparent.

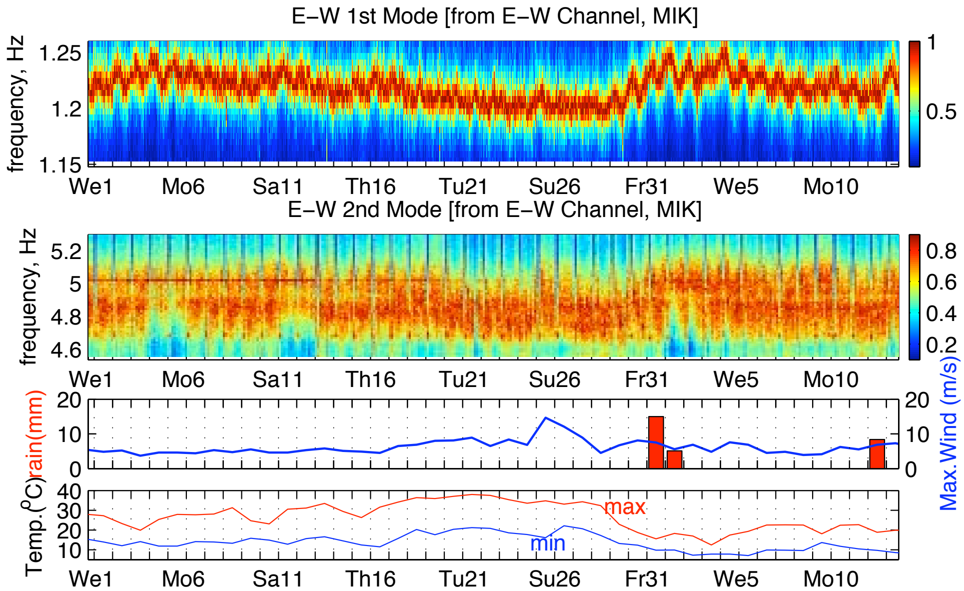

Figure 6.22: Spectrogram plot as Figure 6.20 for October - November 2003, when very hot temperatures and high winds caused widespread forest fires in Southern California, followed by heavy storms and cold weather. Again, note the correlation between rises in natural frequency and heavy rainfall.

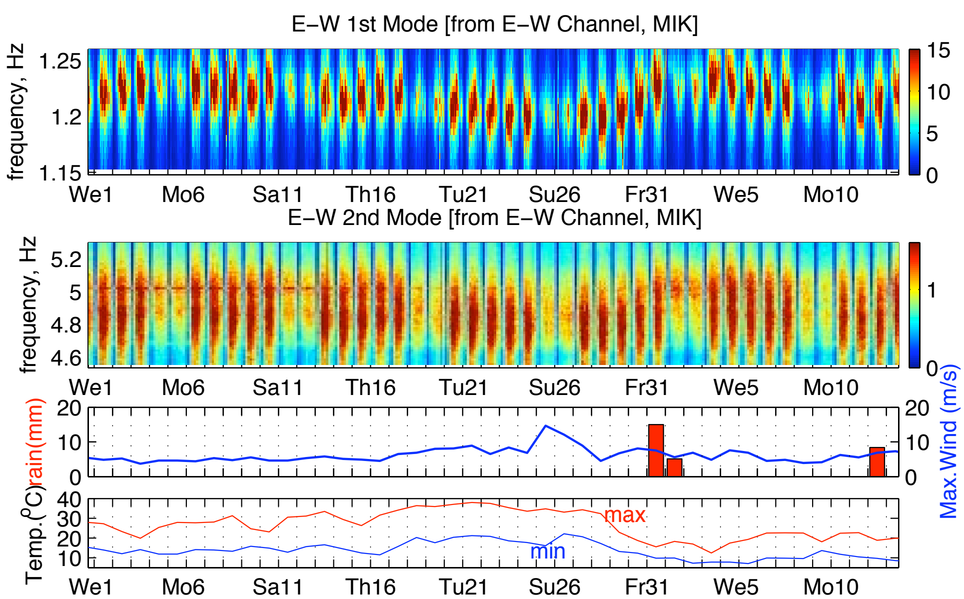

Figure 6.23: As Figure 6.22, with no scaling of each spectrogram, so variations of intensity of each frequency are apparent.

6.4.3 Santa Ana Winds — MIK

Strong winds can also influence the building, though they are usually accompanied with rainfall, which dominates the library's response. Between October and February, dry Easterly Santa Ana winds can affect the Pasadena area. In Figure 6.24, an example of such an intense Santa Ana windstorm (with no rainfall) is presented. The Library shows a sudden, significant drop in all the fundamental frequencies, in particular the E-W mode, which drops by about 3%. Amplitudes of the fundamental modes increase by about an order of magnitude during the windstorm, and the torsional mode increases about $1/2$ as much. Immediately after the event, the stiffness returns to near pre-event levels. This observation is consistent with the drops in natural frequency associated with increasing the weight in force vibration tests, which also increases the amplitude of excitation.

6.4.4 Diurnal Variation and High Temperatures — MIK

Figure 6.25 shows a typical example of the building response during hot weather, when there is significant daily variation of at least 1% for all three fundamental frequencies. This is likely due to both the changing weather conditions, and the daily building usage cycle. The air-conditioning in the building is turned off between the hours of 12pm and 4am, when the library is closed, and the elevators are also not in use. During the evening, the natural frequencies drop, and during the daytime, they increase again. On particularly hot days (such as the 1^{st} and 2^{nd} of September, 2002, in Figure 6.25, where temperatures reach $40^{o}C$), there are higher frequency peaks. On cool, overcast and rainy days (such as in Figure 6.19), this diurnal variation is not as extreme. It is also clear that the torsional mode is more sensitive to temperature than the translational modes - this mode shows large increases in frequency above about $30^{o}C$, whereas the other fundamental frequencies only show frequency increases at temperatures nearing $40^{o}C$. Maximum daily variations can be as large as 3%.

These frequency increases during the day seem to be associated with thermal expansion of the concrete, but as the amplitudes of the ambient motion also increase by an order of magnitude during the day, are inconsistent with the general observation that natural

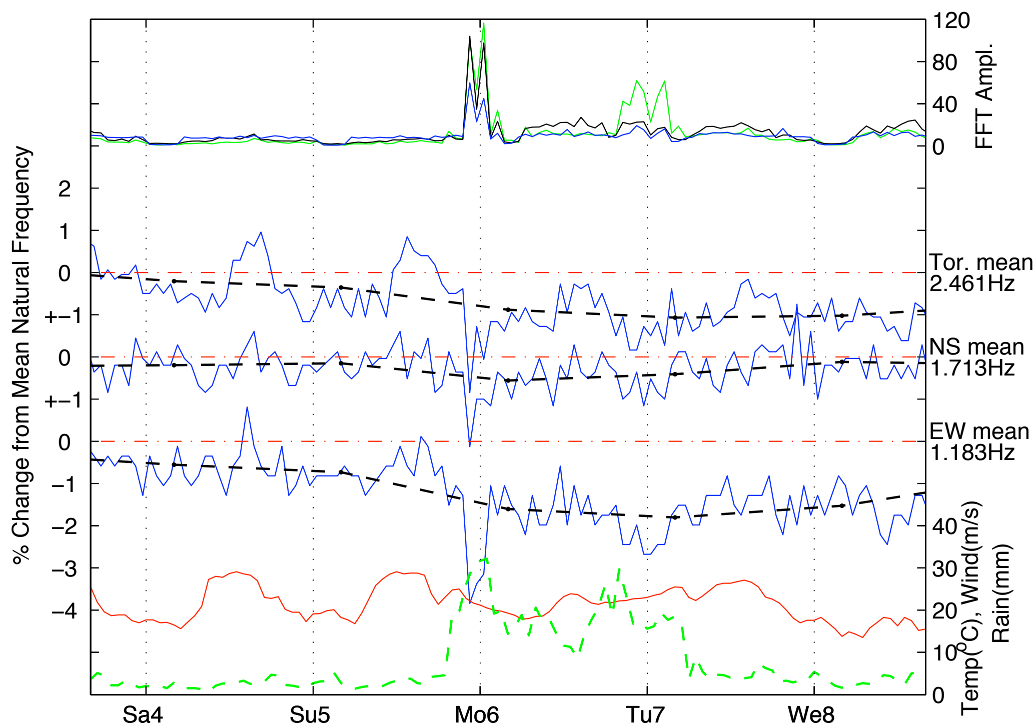

Figure 6.24: As Figure 6.19, for a 5-day period in January 2003, with a particularly intense wind storm (no rainfall). The natural frequencies of the Library dramatically shorten for the duration of the most intense windstorm, most notably in the E-W direction, but also significantly for the N-S and torsional modes. The smaller windstorm in the evening of January 6 appears slightly shifted in time from the response, this may be due to variations in the winds between the Library, and the weather station at JPL. The mean frequencies here are for the month of January.

frequencies drop as amplitude increases. For these amplitude levels, the thermal effects are larger than the excitation amplitude effects.

There does not appear to be any longterm trends associated with seasonal changes in temperature.

Figure 6.25 also includes hourly amplitudes of the FFT peaks, which show increased noise levels in the building associated with the working-hours usage of the building. In the evenings and weekends the building has less noise, as the air-conditioning and other machinery are not in operation.

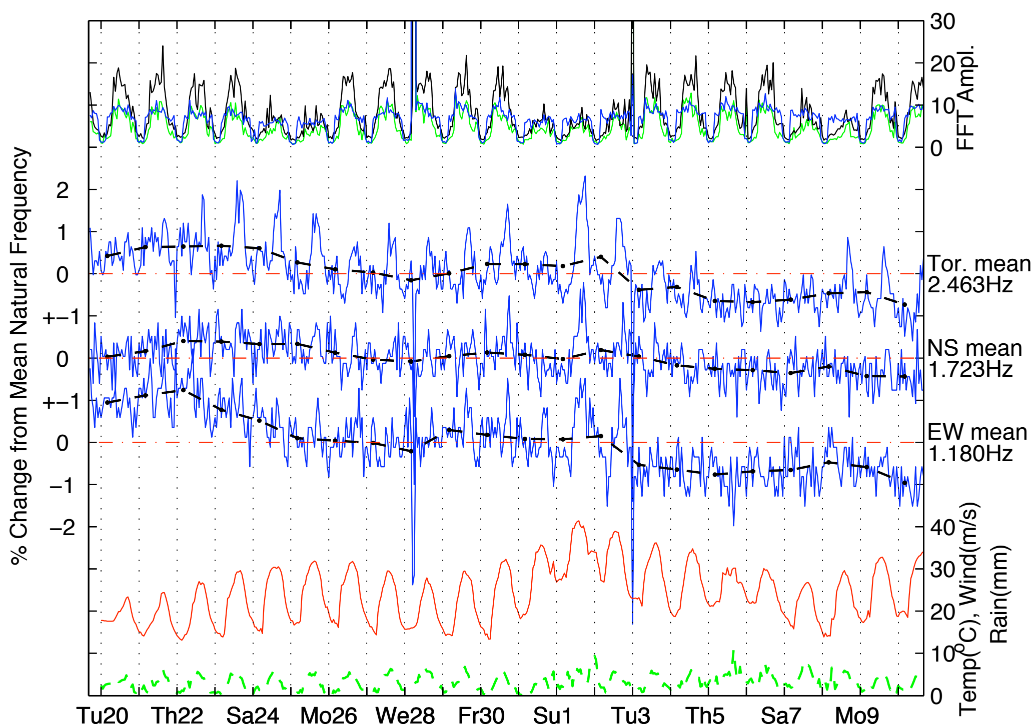

Figure 6.25: As Figure 6.19, for a 22-day period, late August — early September 2002. Typical daily variation during the summer months. Hourly maximum temperatures (solid lines) and the wind gusts (dashed lines) are shown on the bottom [no rainfall]. In the centre of the plot, the hourly smoothed FFT peaks are plotted for the 3 fundamental frequencies. Dashed lines are the daily averages, dashed-dotted lines are the mean for the time period. Above this is plotted the amplitude of the hourly FFT for all 3 fundamental modes. 26Aug: Vibration Testing; 3Sept: M4.8 Yorba Linda earthquake.

6.5 M5.4 22 February 2003 Big Bear Sequence

The moderate M5.4 Big Bear earthquake occurred at 4:19 AM PST on 22 February 2003, at a distance of 120km from the campus. At the time of the event, the stations GSA, MIK and CBC all were operational, and the USGS-Caltech array in Millikan Library also triggered. However, the basement channels and 2 channels recording the N-S directions on the east side of the building did not recover data due to refurbishment of parts of the building.

6.5.1 Millikan Library

USGS Triggered Data - Big Bear Earthquake

Figure 6.26 shows the timeseries for all the E-W channels, and the FFT of the records around the E-W modes: the E-W fundamental frequency is at 1.06Hz and the E-W 2^{nd} mode at 4.55Hz. These values are approximately 7% lower than the corresponding natural frequencies determined during forced vibrations (see Table 6.2). Further, the fundamental frequency is 11% below the ambient natural frequency of 1.19Hz (Figure 6.27) just before the earthquake, and the 2^{nd} mode is 6.2% below the pre-earthquake ambient frequency of 4.85Hz (Figure 6.20).

Note that the amplitude of the peak at 4.55Hz, which is identified as the second mode, is small at the 7^{th}, 8^{th} and 9^{th} floors; the timeseries between 8 and 12 seconds is rich in this frequency in the other floors. If we look at the modeshape for this frequency (see Figure 6.26), these floors are near a nodal point, and this explains why it is difficult to identify the 2^{nd} E-W mode using 9^{th} floor MIK data alone. This is seen in the small magnitude broad 2^{nd} mode peak in Figure 6.21.

Little excitation of other higher order modes was observed in the earthquake data, including the fundamental torsional mode, so no examination of their wander is attempted. Also note that no significant energy is present at the resonant frequencies in the reference site GSA record.

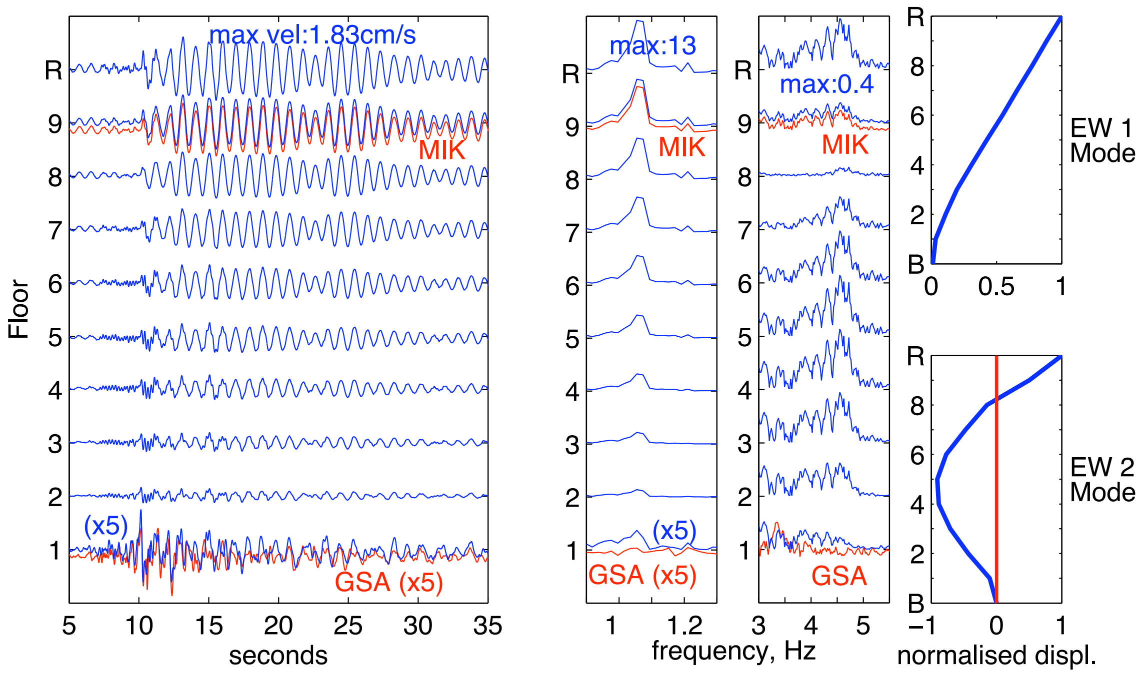

Figure 6.26: East-West components of USGS-Caltech array in Millikan Library, M5.4 Big Bear earthquake - velocity timeseries and FFT. Includes Floors 1-9 and Roof of Millikan Library as well as GSA (‘free-field’ site) and MIK (on 9th floor of Millikan Library), plotted underneath the 1^{st} and 9^{th} channels. FFT plots are centred around the fundamental frequency ($1.06Hz$) and 2^{nd} mode frequency ($4.55Hz$) for the E-W direction. Also included are the modeshapes as identified from forced vibrations *(Bradford et al, 2004)* for the two E-W modes.

MIK Continuous Data: Big Bear Earthquake

The continuously recording strong motion channels from the 9th floor of Millikan provide an excellent opportunity to look at the wander in the Library's natural frequencies before, during and after the mainshock. Also observe how the structure regains its stiffness after minor shaking.

Figure 6.27 shows a spectrogram for the three fundamental frequencies and 2nd E-W mode frequency for a 60 minute period around the mainshock. FFT's are taken over a 30s period with 15s overlap. Although the frequency resolution is poor due to the short FFT length, observe that during the earthquake, the previously relatively stable frequencies all decrease by about 10%. Recovery from the earthquake to pre-earthquake levels appears to be almost instantaneous once the shaking has diminished. Aftershocks also shorten the frequencies, but by a lesser amount, commensurate to the smaller amplitudes of motion — for example, in Figure 6.28, a M4.1 aftershock occurs at 170$mins$, with a measurable decrease in frequency.

Figure 6.28 presents a similar spectrogram as Figure 6.27 for a 3 hour period around the same event, with FFT's taken over a 5 minute period with a 4 minute overlap. This provides improved resolution in the frequency domain, although resolution in the time domain is significantly diminished. The increased length also provides evidence that, though the natural frequencies are shortened a small amount in the immediate aftermath of an event, after about an hour, there is no perceptible difference between the pre- and post-event natural frequencies.

For this level of excitation, the structure regains its stiffness within minutes. This is in contrast to evidence (Udwadia and Trifunac, 1974) that suggests Millikan Library takes weeks or months to return to near pre-earthquake after undergoing strong motion. However, this observation is based on a minor shaking, whereas their observations were from San Fernando earthquake motions, which caused rooftop accelerations over 10 times greater than the Big Bear event. Thus, extrapolation of the Big Bear result to the large shaking that the building has been subjected to may not be valid. Note though that the previous work was based on single tests performed a few weeks and 22-months after the San Fernando earth-

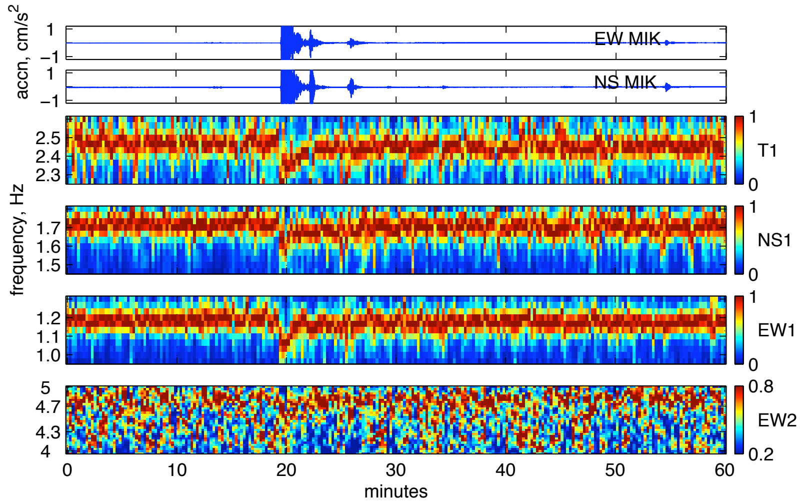

Figure 6.27: Acceleration data and resulting spectrograms for MIK from 12:00GMT to 13:00GMT 22 Feb2003. M5.4 Big Bear earthquake occurs at 12:19GMT. Max accn = 19.3cm/s^2 N-S, 10.9cm/s^2 E-W. Spectrograms are set around the 4 natural frequencies. 30s window spectrograms, with slices shifted by 15s. During the event, the fundamental frequencies shorten considerably during the shaking and aftershocks. Analysis of longterm behaviour, especially that of the 2^{nd} mode E-W, limited by poor resolution due to short FFT length (see Figure 6.28)

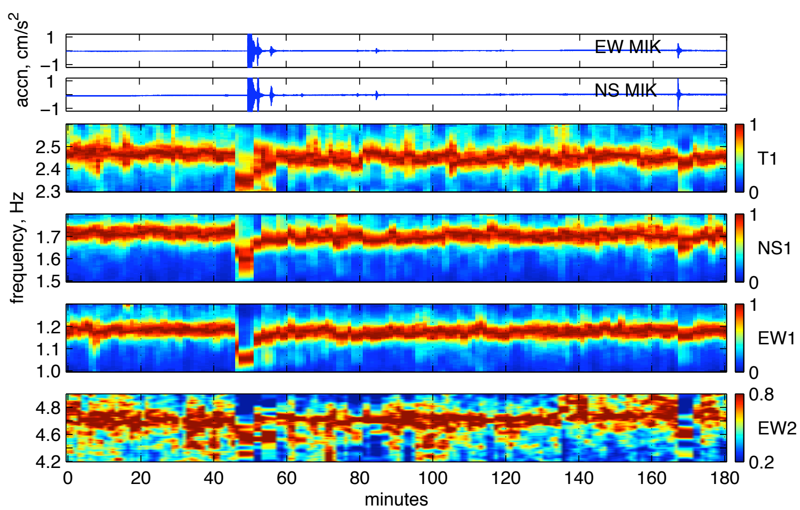

Figure 6.28: As Figure 6.27, but for MIK data from 11:30GMT to 14:30GMT, 5 minute window spectrograms, with slices shifted by 1 minute. M5.4 Big Bear earthquake occurs at 12:19GMT. During the event, as in Figure 6.27, we observe the fundamental frequencies shortening considerably. After shaking, over this time window there is no perceptible longterm shortening of the fundamental frequencies due to the earthquake. The event at 168 minutes is a M4.1 aftershock.

quake, where the observed decreases in the E-W natural frequency from pre-earthquake measurements were 18% and 12% respectively. The Big Bear data suggests the permanent change from the original natural frequency of $1.45Hz$ was about 12%. Udwadia and Trifunac (1974) show FFT segments from the tail of the strong motion record (about $80s$ after the initial triggering) that indicate the building is already returning to the pre-earthquake state. The differences in measurements may be explained by the many changing variables such as weather and test parameters, and may not necessarily be due to longterm 'healing' of the structure.

6.5.2 Broad Center

The continuous data from the Broad Center (CBC) provides another dataset for analysis of the impact of a small earthquake on the natural frequencies of a structure.

Figures 6.29 and 6.30 are 3-hour spectrograms of the 6 horizontal channels of CBC, with FFT's of a length of 5 minutes. These spectrograms have each FFT scaled to a maximum value of 1, so during the earthquake, the torsional mode disappears as the translational modes are predominantly excited. For each channel, a wide frequency band of acceleration spectra is plotted; a narrow band of displacement spectra centred on the fundamental frequency is underneath. Displacement spectra accentuates the energy in this frequency relative to the higher frequencies, and as these two fundamental frequencies are not driven by electrical or mechanical noise, fluctuations in frequency can be more easily observed.

During the earthquake, the natural frequencies all change considerably - it is not clear exactly which frequencies correspond to the values observed during the shaking as all 3 frequencies are so close together. It is clear that immediately after the earthquake, the frequencies return to their pre-earthquake levels.

6.6 A Linear Transfer Function Solution?

A simple method of modeling structural response to ground motions is to convolve the fundamental mode building response with a nearby reference recording of ground motion.

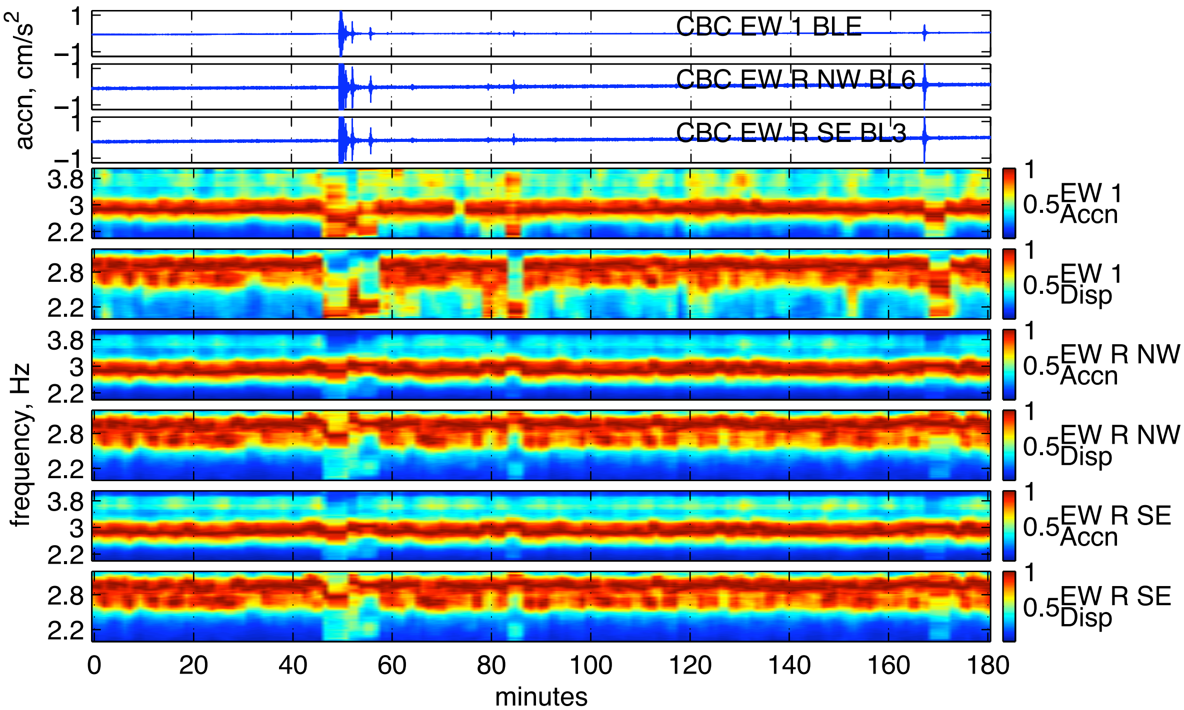

Figure 6.29: CBC E-W channels - acceleration timeseries and spectrograms from 11:30GMT to 14:30GMT, with FFT slices of 5 minutes length with each slice shifted by 1 minute. There are two spectrograms for each E-W channel — the first is a broad frequency range from acceleration data showing all identified modal frequencies. The second is a frequency band around the first mode only from displacement data to accentuate the behaviour of this the only mode without nearby machine noise (see Figure 6.13). M5.4 Big Bear earthquake occurs at 12:19GMT. Max accn = 14.8cm/s^2 at BL6, NW Roof. During the event, observe the fundamental frequencies shortening considerably. After shaking, over this time window there is no perceptible longterm shortening of the fundamental frequencies due to the earthquake.

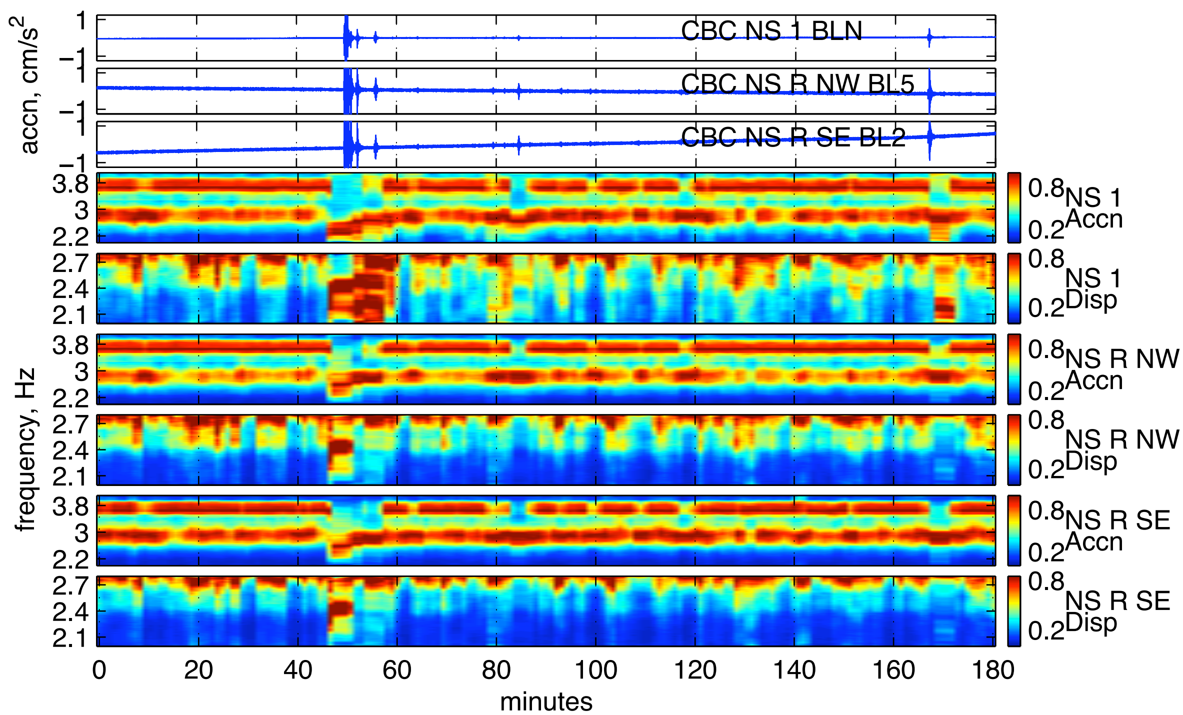

Figure 6.30: as Figure 6.29 — for CBC N-S channels. Max accn = $16.2 cm/s^2$ at BL5, NW Roof

There are obvious problems with this linear method during strong motion, since the fundamental frequency varies with excitation levels. Nonetheless, during small excitations, a linear response is expected.

A simple model is used which convolves the E-W acceleration ground motion at GSA with an impulse response of a single degree of freedom (SDOF) model representing the E-W fundamental frequency of Millikan Library. Amplitude amplification is determined using the participation factor of the first mode, assuming a mass matrix of equal floor mass, and modeshapes as determined from the forced vibration tests. This convolution gives the relative displacement of MIK to GSA, so we add to this the ground displacement at GSA. A constant damping ratio of 1.63% is employed, which is the value determined during the forced vibration tests (Bradford et al., 2004).

Figures 6.31 and 6.32 are examples of the results for 2 recent earthquakes. Figure 6.31 presents data from the 18 June 2003 M2.0 Pasadena earthquake (a foreshock of the bigger M2.6 event), $5km$ from Caltech, which had a maximum acceleration of $1.2cm/s^2$ at MIK. Figure 6.32 presents data from the 22 February 2003 M5.4 Big Bear earthquake, $119km$ from Caltech, which had a maximum acceleration of $22.6cm/s^2$ at MIK. Figure 6.31 shows that the model is improved if the ambient SDOF is used instead of the default forced vibration value (Note for this event, a default SDOF representing the second E-W mode is also included to help model the high frequency response). In Figure 6.32, where the behaviour of Millikan during the stronger motion is modelled, both the ambient and forced SDOF give a poor fit. In this case, the natural frequency has moved far from the ambient levels (as seen in Figure 6.26), and is best modelled using a natural frequency as determined from the strong motion records ($1.06Hz$). Note that though the character of the strongest motions is well modelled by this last SDOF, the low amplitude P-wave and coda motions are not well modelled as the natural frequency of the building seems to be evolving rapidly, as the excitation amplitude changes. These motions are small, and are certainly within what we would expect the linear response of the building, yet a single natural frequency cannot predict the motions of the building.

Current engineering practice has a single natural frequency assigned to the building, usually not even derived from experimental testing, but from formulae in the relevant design code. This natural frequency is assumed constant for a wide range of ground motions. This data suggests this may not be the case even for weak motions.

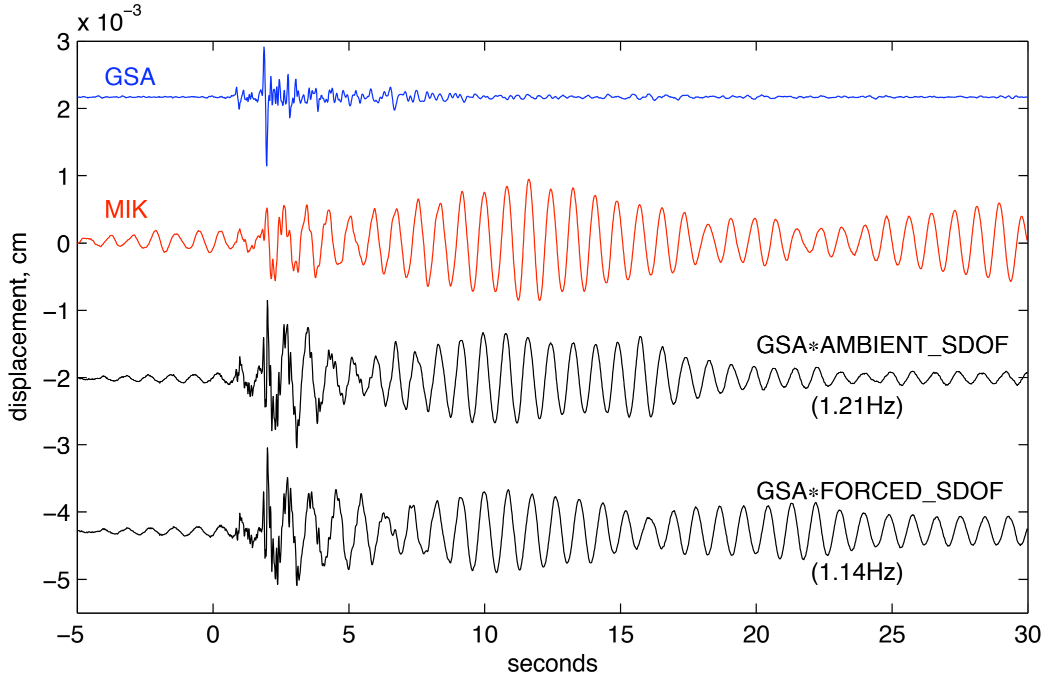

Figure 6.31: Prediction of MIK E-W motions using GSA E-W as input motion, for the M2.0 18 June 2003 Pasadena earthquake ($\Delta = 5km$). Motions recorded at GSA are convolved with an impulse response at a particular frequency. Damping is held constant at 1.63%. **Ambient_SDOF** uses the fundamental frequency as determined from FFT's of pre-event data ($1.21Hz$), **Forced_SDOF** uses the fundamental frequency as determined from Forced Vibration tests ($1.14Hz$). A 2^{nd} mode SDOF response is included for both models to reflect the high frequency components of the motions. During this very small amplitude motion, the natural frequency determined using the ambient data models the observations at MIK better than the forced vibration result.

6.7 Conclusions and Discussion

The data presented herein indicates that the dynamic behaviour of Millikan Library is determined by several external factors on very different timescales. There is significant wander in the translational and torsional natural frequencies of the structure. The determination of these frequencies is very dependent on the method/data used to estimate this frequency — whether we use ambient data, forced vibration data, or earthquake records.

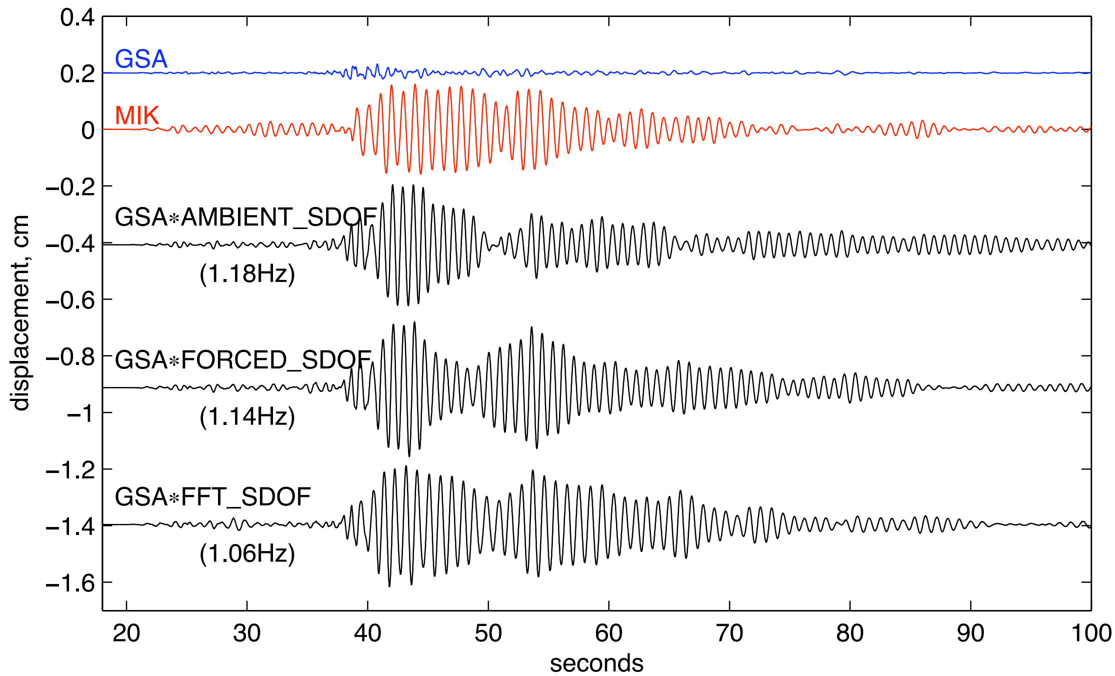

Figure 6.32: Prediction of MIK E-W motions using GSA E-W as input motion, for the M5.4 22 February 2003 Big Bear earthquake ($\Delta = 119km$). As Figure 6.31, with the **Ambient_SDOF** at $1.18Hz$, and **Forced_SDOF** at $1.14Hz$. Neither of these model the MIK observation well, so we include another SDOF, **FFT_SDOF**, with natural frequency at $1.06Hz$, as determined by the FFT peak of the strong motion record. This leads to a somewhat model of the observed motion. This shows that even during the moderate shaking generated from this relatively small and distant earthquake, a linear building model is inappropriate. A model that can have evolving natural frequencies will best represent the observed motions.

To the first order, there has been a significant permanent reduction in natural frequencies for the Millikan Library in the 36 years of its life, 22% E-W and 12% N-S. As the system mass did not change much during the lifespan [and removing the entire book collection from 3 of the lower floors is not shown to have an observable effect], this corresponds to a major decrease in system stiffness.

The large permanent frequency drops appear to be almost entirely caused by strong motions from moderate nearby LA Basin earthquakes. In particular, the 1971 San Fernando M6.6 earthquake had the largest effect, with permanent drops of 17% E-W and 7% N-S. For the E-W direction, the accelerations of this earthquake were not subsequently exceeded, and there are no more large permanent frequency drops. However, in the N-S direction, the San Fernando roof-top acceleration of $341 cm/s^2$ was exceeded with a recording of $534 cm/s^2$ during the 1987 M6.1 Whittier Narrows event. This caused a further permanent offset of 4%.

During the strong shaking, these moderate local events are shown to almost instantaneously shorten the frequencies by over 20%, without apparent structural damage. As there is only triggered data available, there is no clear evidence of the time-frame of stiffness recovery.

Smaller transient excitations also reduce the natural frequencies, such as forced shaking tests (by up to 7% with full shaker weights) and small earthquakes. Heavy rain can be seen to increase the E-W fundamental and 2^{nd} mode frequencies, and the torsional fundamental frequencies by up to 3% in a matter of hours, with little effect to the N-S fundamental frequency. Conversely, strong winds diminish all the natural frequencies by up to 3%, with inverse correlation with amplitude. The diurnal variation is of the order of $1-2\%$. On a day with a high temperatures near 40^oC, rising temperatures raise all the natural frequencies by a further $1-2\%$.

The recovery from these transient changes also varies. Certain moderate earthquakes have been shown to permanently shorten the observed frequencies - the 1971 M6.6 San Fernando event temporarily shortened the E-W fundamental frequency by 31%, and permanently by 16%. Subsequent earthquakes with similar ground motion magnitudes have also permanently reduced natural frequencies by a few percent. Small earthquake motions, such as from the 2003 M5.4 Big Bear earthquake, reduce the ambient natural frequencies by 10% during the motion, with a full recovery within minutes. Similar observations are documented for the fundamental translational modes of the Broad Center.

For changes due to extreme weather, the recovery time can vary significantly. Any changes arising from wind and temperature only seem to last as long as the excitation, but for rain events the Library and the Broad Center slowly return to the pre-event fundamental frequencies over a time-span of about 1 week.

On a longer timescale, changing building usage can be responsible for large changes in the frequencies. Construction of partition walls to provide office space in 3 mid-level floors of the library over the period of 4-months is shown to coincide with an increase in frequencies during this same period — the E-W fundamental frequency is particular affected (4% increase over this period). It is noted that a 4% increase in natural frequency corresponds to a 8% increase in stiffness for the whole structure. This large stiffness increase cannot be realistically explained solely by placing partition walls in three middle floors.

The sources of all these observed wanders are not well understood. The different observed effects may be due to soil-structure interaction, super-structure non-linearities, or a combination of both.

For the particular case of Millikan Library, Chopra (1995) suggests that the the changes in the dynamic behaviour of the building during strong motion and weak forced shaking are associated with 'cracking and other types of degradation of the so-called non-structural elements'. This mechanism does not account for the observed changes due to weather events.

The increases in natural frequency, and thus apparent increase in stiffness, during rain events may be caused by saturation of the soil. Though this could reduce the frictional resistance between the concrete and the soil at the foundation, which would lead to a more compliant system, reducing the natural frequencies. If the soil is dry before the event, saturation could also cause swelling of the soil, producing extra pressure against the sides of the foundations, reducing the amount of rocking and translation of the building. This attenuation of the base motions would lead to a stiffer system. Unfortunately, this does not explain why the E-W mode is most affected by the weather, but has very little rocking component to its modeshape, yet the N-S mode, with 30% of the roof displacement for this modeshape being due to basement rocking (Appendix 3, Bradford et al, 2004), is not affected as much. Further, the gardens surrounding the building are heavily watered through out the year, so are likely to be near saturated year round. It is also noted the natural frequencies rise as soon as the rainfall event begins, or even beforehand. This could be due to to the fact the building is sensitive to pressure variations, but more likely it is because JPL weather station is $7km$ distant from Caltech, towards the mountains, and may receive its rainfall slightly delayed to to th Caltech Campus.

Stiffness changes in the super-structure during rain events should also be considered. Wetting of the concrete could potentially lead to expansion of the window/wall panels, and thus stiffen the E-W moment frames. This would explain why the E-W mode is most affected by rainfall. Slow recovery of pre-event stiffnesses would be determined by the drying process, which would be slow in the winter rainy season. Cycles of heating and cooling could have the same effect on the super-structure, but as heat is radiated quickly, this effect is transient.

Both mechanisms explain the observation that large rains not preceded by other events cause the largest increases in natural frequency. Rainfall events which closely follow the large events do not cause major changes themselves, as the soil or concrete is already in an expanded state.

The loss of natural frequency during heavy winds is consistent with the observations from previous investigators that as the amplitude of forced vibrations increases, the frequency drops. This is also consistent with the drop of frequency with increasing amplitude of earthquake excitation, from weak motions to strong motions, presented here.

The rise in frequency during hot weather is likely due to thermal expansion of the concrete stiffening the frame. All three fundamental frequencies are similarly affected by this. During the day, the ambient excitation is an order of magnitude larger than at night (when elevators and air conditioning are not in use, and the building is un-occupied), and so in the absence of this thermal expansion, the natural frequencies during the day would be expected to decrease.

The dramatic reduction in stiffness during moderate shaking could also be due to non-linear soil-structure interaction - as there is no appreciable structural damage to Millikan during strong shaking. Measurement of pore-water pressures near the Library would help resolve the validity of this hypothesis. Another explanation would be that the bolted wall panels on the North and South sides of the structure, which provide resistance in the East-West direction, may loosen during stronger shaking. A single crack has been observed along pour lines on the North-South elevator core shear wall between the basement and 1^{st} floor, and between the 1^{st} and 2^{nd} floors. Analysis of strain over the length of these cracks during different motions may also give insight into whether the loss of stiffness observed in the building may be due to rocking about these cracks. Potentially there are other cracks in the elevator core in the East-West walls, but these walls are covered by architectural features, and cannot be investigated.

The wandering in the natural frequencies is significant for the engineering community. In engineering practice, a linear structural behaviour is assumed for ambient and small motions, but this is clearly not the case. Further, as real-time structural health monitoring is becoming a reality, these unexpectedly large variations in the fundamental parameter of building response need to be accounted for in any damage assessment. Structural damage usually results in a loss in structural stiffness, which is characterised by a drop in the natural frequency. However, these observations of wandering natural frequencies due to ambient and small motions should serve to caution us that not all changes in natural frequency can be attributed to structural damage. This phenomena needs to be accounted for by any damage assessment methodology with any claims of robustness.